ISSN 1948-9358 (online)

World Journal of *Diabetes*

World J Diabetes 2024 July 15; 15(7): 1384-1653

Published by Baishideng Publishing Group Inc

World Journal of Diabetes

Contents

Monthly Volume 15 Number 7 July 15, 2024

EDITORIAL

1384 Remission of type 2 diabetes mellitus

Nakhleh A, Halfin E, Shehadeh N

1390 Diabetes remission and nonalcoholic fatty pancreas disease

Wu WJ

1394 Management of gestational diabetes mellitus *via* nutritional interventions: The relevance of gastric emptying

Huang WK, Jalleh RJ, Rayner CK, Wu TZ

1398 MicroRNA-630: A promising avenue for alleviating inflammation in diabetic kidney disease

Donate-Correa J, González-Luis A, Díaz-Vera J, Hernandez-Fernaud JR

1404 Adiposity in Chinese people with type 1 diabetes

Wu NW, Lyu XF, An ZM, Li SY

1409 Diabetes and tuberculosis: An emerging dual threat to healthcare

Shetty S, Pappachan JM, Fernandez CJ

REVIEW

1417 Patient-centered care in diabetes care-concepts, relationships and practice

Chen TT, Su WC, Liu MI

1430 Insulin resistance as the molecular link between diabetes and Alzheimer's disease

Abdalla MMI

MINIREVIEWS

1448 Obstructive sleep apnea: Overlooked comorbidity in patients with diabetes

Tenda ED, Henrina J, Cha JH, Triono MR, Putri EA, Aristy DJ, Tahapary DL

1461 Update on evidence-based clinical application of sodium-glucose cotransporter inhibitors: Insight to uncommon cardiovascular disease scenarios in diabetes

Tao SB, Lu X, Ye ZW, Tong NW

World Journal of Diabetes

Monthly Volume 15 Number 7 July 15, 2024

Contents

ORIGINAL ARTICLE

Retrospective Cohort Study

1477 Association between glucose levels of children with type 1 diabetes and parental economic status in mobile health application

Zhang WH, Wang CF, Wang H, Tang J, Zhang HQ, Zhu JY, Zheng XY, Luo SH, Ding Y

Retrospective Study

1489 Association between glucose-lowering drugs and circulating insulin antibodies induced by insulin therapy in patients with type 2 diabetes

Zhang P, Jiang Q, Ding B, Yan RN, Hu Y, Ma JH

1499 Clinical efficacy of endovascular revascularization combined with vacuum-assisted closure for the treatment of diabetic foot

Lei FR, Shen XF, Zhang C, Li XQ, Zhuang H, Sang HF

1509 Magnetic resonance imaging combined with serum endolipin and galactagoglobin-3 to diagnose cerebral infarction in the elderly with diabetes mellitus

Zhang YH, Liang D

1518 Dapagliflozin in heart failure and type 2 diabetes: Efficacy, cardiac and renal effects, safety

Yu PL, Yu Y, Li S, Mu BC, Nan MH, Pang M

Observational Study

1531 Cut-off value of glycated hemoglobin A1c for detecting diabetic retinopathy in the Chinese population

Wen Y, Wang Q

1537 Glymphatic function and its influencing factors in different glucose metabolism states

Tian B, Zhao C, Liang JL, Zhang HT, Xu YF, Zheng HL, Zhou J, Gong JN, Lu ST, Zeng ZS

Clinical and Translational Research

1551 Does type 1 diabetes serve as a protective factor against inflammatory bowel disease: A Mendelian randomization study

Tong KK, Yu YF, Yang XY, Wu JY, Yu R, Tan CC

1562 Network pharmacology and molecular dynamics study of the effect of the *Astragalus-Coptis* drug pair on diabetic kidney disease

Zhang MY, Zheng SQ

Basic Study

1589 Interactions between myoblasts and macrophages under high glucose milieus result in inflammatory response and impaired insulin sensitivity

Luo W, Zhou Y, Wang LY, Ai L

World Journal of Diabetes

Monthly Volume 15 Number 7 July 15, 2024

Contents

SYSTEMATIC REVIEWS

1603 Natural product-based treatment potential for type 2 diabetes mellitus and cardiovascular disease

Shrivastav D, Kumbhakar SK, Srivastava S, Singh DD

META-ANALYSIS

1615 Evaluation of teplizumab's efficacy and safety in treatment of type 1 diabetes mellitus: A systematic review and meta-analysis

Ma XL, Ge D, Hu XJ

SCIENTOMETRICS

1627 Global trends in publications regarding macrophages-related diabetic foot ulcers in the last two decades

Wen JP, Ou SJ, Liu JB, Zhang W, Qu YD, Li JX, Xia CL, Yang Y, Qi Y, Xu CP

LETTER TO THE EDITOR

1645 Atrial fibrillation and prediabetes: A liaison that merits attention!

Batta A, Hatwal J

1648 Serum tumor markers: Can they clinically implicate in type 2 diabetes mellitus?

Reddy KS, Pandiaraj IP, Gaur A, Varatharajan S

1651 Bidirectional link between periodontitis and systemic inflammation in diabetic retinopathy

Nishant P, Sinha S, Sinha RK, Morya AK

ABOUT COVER

Peer Review of *World Journal of Diabetes*, Erkan Gokce, MD, Professor, Department of Radiology, Tokat Gaziosmanpasa University, School of Medicine, Tokat 60100, Türkiye. drerkangokce@gmail.com

AIMS AND SCOPE

The primary aim of *World Journal of Diabetes* (*WJD*, *World J Diabetes*) is to provide scholars and readers from various fields of diabetes with a platform to publish high-quality basic and clinical research articles and communicate their research findings online.

WJD mainly publishes articles reporting research results and findings obtained in the field of diabetes and covering a wide range of topics including risk factors for diabetes, diabetes complications, experimental diabetes mellitus, type 1 diabetes mellitus, type 2 diabetes mellitus, gestational diabetes, diabetic angiopathies, diabetic cardiomyopathies, diabetic coma, diabetic ketoacidosis, diabetic nephropathies, diabetic neuropathies, Donohue syndrome, fetal macrosomia, and prediabetic state.

INDEXING/ABSTRACTING

The *WJD* is now abstracted and indexed in Science Citation Index Expanded (SCIE, also known as SciSearch®), Current Contents/Clinical Medicine, Journal Citation Reports/Science Edition, PubMed, PubMed Central, Reference Citation Analysis, China Science and Technology Journal Database, and Superstar Journals Database. The 2024 Edition of Journal Citation Reports® cites the 2023 journal impact factor (JIF) for *WJD* as 4.2; JIF without journal self cites: 4.1; 5-year JIF: 4.2; JIF Rank: 40/186 in endocrinology and metabolism; JIF Quartile: Q1; and 5-year JIF Quartile: Q2.

RESPONSIBLE EDITORS FOR THIS ISSUE

Production Editor: *Yu-Xi Chen*; **Production Department Director:** *Xu Guo*; **Cover Editor:** *Jia-Ru Fan*.

NAME OF JOURNAL
World Journal of Diabetes

ISSN
ISSN 1948-9358 (online)

LAUNCH DATE
June 15, 2010

FREQUENCY
Monthly

EDITORS-IN-CHIEF
Lu Cai, Md. Shahidul Islam, Michael Horowitz

EDITORIAL BOARD MEMBERS
https://www.wjgnet.com/1948-9358/editorialboard.htm

PUBLICATION DATE
July 15, 2024

COPYRIGHT
© 2024 Baishideng Publishing Group Inc

INSTRUCTIONS TO AUTHORS
https://www.wjgnet.com/bpg/gerinfo/204

GUIDELINES FOR ETHICS DOCUMENTS
https://www.wjgnet.com/bpg/GerInfo/287

GUIDELINES FOR NON-NATIVE SPEAKERS OF ENGLISH
https://www.wjgnet.com/bpg/gerinfo/240

PUBLICATION ETHICS
https://www.wjgnet.com/bpg/GerInfo/288

PUBLICATION MISCONDUCT
https://www.wjgnet.com/bpg/gerinfo/208

ARTICLE PROCESSING CHARGE
https://www.wjgnet.com/bpg/gerinfo/242

STEPS FOR SUBMITTING MANUSCRIPTS
https://www.wjgnet.com/bpg/GerInfo/239

ONLINE SUBMISSION
https://www.f6publishing.com

© 2024 Baishideng Publishing Group Inc. All rights reserved. 7041 Koll Center Parkway, Suite 160, Pleasanton, CA 94566, USA
E-mail: office@baishideng.com https://www.wjgnet.com

World Journal of Diabetes

Submit a Manuscript: https://www.f6publishing.com

World J Diabetes 2024 July 15; 15(7): 1562-1588

DOI: 10.4239/wjd.v15.i7.1562

ISSN 1948-9358 (online)

ORIGINAL ARTICLE

Clinical and Translational Research

Network pharmacology and molecular dynamics study of the effect of the *Astragalus-Coptis* drug pair on diabetic kidney disease

Mo-Yan Zhang, Shu-Qin Zheng

Specialty type: Endocrinology and metabolism

Provenance and peer review: Unsolicited article; Externally peer reviewed.

Peer-review model: Single blind

Peer-review report's classification

Scientific Quality: Grade B, Grade B, Grade C, Grade C

Novelty: Grade B, Grade B

Creativity or Innovation: Grade B, Grade B

Scientific Significance: Grade B, Grade B

P-Reviewer: Alsindi N, United Arab Emirates; Pennazio M, Italy

Received: April 3, 2024

Revised: May 13, 2024

Accepted: May 29, 2024

Published online: July 15, 2024

Processing time: 95 Days and 16.3 Hours

Mo-Yan Zhang, Liaoning University of Traditional Chinese Medicine, Liaoning University of Traditional Chinese Medicine, Shenyang 110847, Liaoning Province, China

Shu-Qin Zheng, Department of Endocrinology, The Affiliated Hospital of Liaoning University of Traditional Chinese Medicine, Shenyang 110032, Liaoning Province, China

Corresponding author: Shu-Qin Zheng, MSc, Associate Professor, Department of Endocrinology, The Affiliated Hospital of Liaoning University of Traditional Chinese Medicine, No. 33 Beiling Street, Huanggu District, Shenyang 110032, Liaoning Province, China. qxjzsq@sina.com

Abstract

BACKGROUND

Diabetic kidney disease (DKD) is the primary cause of end-stage renal disease. The *Astragalus-Coptis* drug pair is frequently employed in the management of DKD. However, the precise molecular mechanism underlying its therapeutic effect remains elusive.

AIM

To investigate the synergistic effects of multiple active ingredients in the *Astragalus-Coptis* drug pair on DKD through multiple targets and pathways.

METHODS

The ingredients of the *Astragalus-Coptis* drug pair were collected and screened using the TCMSP database and the SwissADME platform. The targets were predicted using the SwissTargetPrediction database, while the DKD differential gene expression analysis was obtained from the Gene Expression Omnibus database. DKD targets were acquired from the GeneCards, Online Mendelian Inheritance in Man database, and DisGeNET databases, with common targets identified through the Venny platform. The protein-protein interaction network and the "disease-active ingredient-target" network of the common targets were constructed utilizing the STRING database and Cytoscape software, followed by the analysis of the interaction relationships and further screening of key targets and core active ingredients. Gene Ontology (GO) function and Kyoto Encyclopedia of Genes and Genomes (KEGG) pathway enrichments were performed using the DAVID database. The tissue and organ distributions of key targets were evaluated. PyMOL and AutoDock software validate the molecular docking between the core ingredients and key targets. Finally, molecular dynamics (MD)

simulations were conducted to simulate the optimal complex formed by interactions between core ingredients and key target proteins.

RESULTS

A total of 27 active ingredients and 512 potential targets of the *Astragalus-Coptis* drug pair were identified. There were 273 common targets between DKD and the *Astragalus-Coptis* drug pair. Through protein-protein interaction network topology analysis, we identified 9 core active ingredients and 10 key targets. GO and KEGG pathway enrichment analyses revealed that *Astragalus-Coptis* drug pair treatment for DKD involves various biological processes, including protein phosphorylation, negative regulation of apoptosis, inflammatory response, and endoplasmic reticulum unfolded protein response. These pathways are mainly associated with the advanced glycation end products (AGE)-receptor for AGE products signaling pathway in diabetic complications, as well as the Lipid and atherosclerosis. Molecular docking and MD simulations demonstrated high affinity and stability between the core active ingredients and key targets. Notably, the quercetin-AKT serine/threonine kinase 1 (AKT1) and quercetin-tumor necrosis factor (TNF) protein complexes exhibited exceptional stability.

CONCLUSION

This study demonstrated that DKD treatment with the *Astragalus-Coptis* drug pair involves multiple ingredients, targets, and signaling pathways. We propose a novel approach for investigating the molecular mechanism underlying the therapeutic effects of the *Astragalus-Coptis* drug pair on DKD. Furthermore, we suggest that quercetin is the most potent active ingredient and specifically targets AKT1 and TNF, providing a theoretical foundation for further exploration of pharmacologically active ingredients and elucidating their molecular mechanisms in DKD treatment.

Key Words: *Astragalus membranaceus*; *Coptis chinensis* Franch; Diabetic kidney disease; Network pharmacology; Molecular docking; Molecular dynamics simulation

©The Author(s) 2024. Published by Baishideng Publishing Group Inc. All rights reserved.

Core Tip: Network pharmacology, molecular docking, and molecular dynamics simulation studies have demonstrated that diabetic kidney disease (DKD) treatment with the *Astragalus-Coptis* drug pair involves a diverse range of active ingredients, targets, and pathways. Additionally, quercetin has been found to exhibit strong affinity and binding stability with AKT serine/threonine kinase 1 and tumor necrosis factor, highlighting its potential therapeutic role in DKD. The findings of this study establish a robust theoretical basis for applying the *Astragalus-Coptis* drug pair in DKD treatment, and these results may provide a guiding framework for further experiments.

Citation: Zhang MY, Zheng SQ. Network pharmacology and molecular dynamics study of the effect of the *Astragalus-Coptis* drug pair on diabetic kidney disease. *World J Diabetes* 2024; 15(7): 1562-1588
URL: https://www.wjgnet.com/1948-9358/full/v15/i7/1562.htm
DOI: https://dx.doi.org/10.4239/wjd.v15.i7.1562

INTRODUCTION

Diabetic kidney disease (DKD) is a form of chronic kidney disease that arises as a consequence of diabetes mellitus and is the primary etiology of end-stage renal disease (ESRD)[1]. Approximately 40% of patients with type 2 diabetes and approximately 30% of patients with type 1 diabetes are prone to developing DKD[2]. As the prevalence of diabetes increases globally, the number of people with DKD is expected to increase by nearly 50% over the next 24 years, from 537 million to 783 million[3]. The pathogenesis of DKD is associated with alterations in renal hemodynamics, oxidative stress, inflammation, renal fibrosis, hypoxia, and hyperactivity of the renin-angiotensin-aldosterone system[4,5]. The current approach to managing DKD primarily revolves around glycemic control and rigorous antihypertensive therapy; however, it fails to effectively halt the progression of DKD to ESRD. The treatment options for end-stage renal failure, such as dialysis and kidney transplantation, are burdened by high costs, frequent adverse reactions, and limited availability of renal sources[6-8].

Traditional Chinese medicine (TCM) has a rich history spanning thousands of years, rendering it uniquely advantageous for ameliorating the clinical symptoms and indicators exhibited by patients with DKD. Consequently, TCM is an indispensable intervention method for the clinical prevention and treatment of this disease[9,10]. The pathogenesis of DKD is relatively intricate. Modern TCM succinctly characterizes it as the syndrome of "deficiency in origin and excess in superficiality". Several studies have demonstrated that the "deficiency in origin" of DKD is primarily characterized by Qi deficiency, while the "excess in superficiality" is dominated by heat. Among these, *Astragalus* (*Astragalus membranaceus*. Huang Qi) and *Coptis* (*Coptis chinensis* Franch. Huang Lian) are commonly used for invigorating Qi and clearing heat,

respectively[11]. *Astragalus* was initially described in Benjing (*Sheng Nong's herbal classic*) for its functions in tonifying Qi, elevating Yang, consolidating surface and antiperspirant effects, reducing edema, and promoting diuresis, nourishing body fluids and enriching the blood. *Coptis* is first mentioned in Benjing, highlighting its therapeutic properties, such as heat-clearing and dampness-drying effects, fire-reducing capabilities and detoxification abilities. The antioxidative stress, inhibitory response to inflammation, regulation of glucose and lipid metabolism, protection of podocytes, and enhancement of insulin sensitivity exhibited by *Astragalus* can effectively attenuate renal function deterioration in patients with DKD[12]. The administration of *Coptis* exerts a significant impact on glycemic control, blood pressure regulation, lipid metabolism disorder correction, and proteinuria reduction in patients with DKD, thereby effectively delaying disease progression[13]. The compatibility of *Astragalus* and *Coptis* aligns with the therapeutic principle of "supplementing deficiency and reducing actual symptoms" in the *Sanbu Jiu hou Lun of Plain Questions*, as both herbs serve to tonify Qi and reduce fire. The *Astragalus-Coptis* drug pair has demonstrated significant efficacy in DKD clinical treatment. However, there is a lack of comprehensive investigations into its beneficial effects on DKD mechanisms, including analyses of its active ingredients and targets, biological processes (BP), and pathways.

Network pharmacology (NP) is an emerging discipline rooted in the principles of systems biology and is employed for identifying targets within TCM ingredients. Aligned with the holistic approach of TCM in treating diseases through multiple ingredients, targets, and pathways, NP enables a comprehensive assessment of drug regulatory effects on biomolecular networks from a systemic perspective. This novel paradigm offers insights into and visualizations of the potential interaction network between TCM and multifactorial diseases[14,15]. The application of molecular docking techniques enables the evaluation of binding surfaces and interaction forces between receptors and ligands, as well as the prediction of binding modes and affinities in receptor-ligand complexes[16]. The structural stability and flexibility of the receptor and ligand, as well as the dynamics of receptor-ligand interactions based on appropriate force fields, are assessed through molecular dynamics (MD) simulations[17].

The present study employed NP to investigate the synergistic effects of multiple active ingredients in the *Astragalus-Coptis* drug pair on DKD through multiple targets and pathways. Molecular docking technology and MD simulation were employed to validate the results, providing a theoretical basis for subsequent traditional Chinese medicine treatment of DKD and novel drug development.

MATERIALS AND METHODS

Identification of the active ingredients and targets of the Astragalus-Coptidis drug pair

The TCMSP is a highly authoritative platform in Chinese herbal medicine system pharmacology that facilitates the screening of active ingredients in drugs and the analysis of the relationships between drug targets and diseases[18]. The active ingredients were queried in the TCMSP database using "Huangqi" and "Huanglian" as search terms. TCM is primarily administered orally and exerts its effects through gastrointestinal digestion and absorption, blood circulation, and metabolism. Therefore, it is essential to evaluate the absorption, distribution, metabolism, and excretion (ADME) properties of the retrieved active ingredients. The retrieval results were filtered based on the criteria of oral bioavailability (OB) ≥ 30% and drug-likeness (DL) ≥ 0.18[19]. The active ingredients were imported from the PubChem database and Novopro platform, consistent with the standard. Canonical SMILESs for each ingredient were obtained and subsequently entered into the SwissADME platform[20]. The GI absorption score was classified as "high". The screening criteria based on the Lipinski, Ghose, Veber, Egan, and Muegge rules required at least two positive results ("Yes") for DL. The results were collected and imported into the SwissTargetPrediction database, where "*Homo sapiens*" was selected as the target species. Predictions of targets for each active ingredient were made, and target data with a probability greater than 0.1 were compiled. The URLs for the database and platform mentioned in this article are presented in Table 1.

Identification of common targets between DKD targets and active ingredient targets

The Human Gene Database (GeneCards)[21], the Online Mendelian Inheritance in Man database (OMIM)[22], and the DisGeNET platform[23] were utilized to search for "Diabetic Kidney Disease" and "Diabetic Nephropathy" as keywords. The targets obtained from these three databases were then consolidated, eliminating any duplicates, to obtain the targets related to DKD. The Venny2.1 platform was used to identify common targets by identifying the intersection of targets for active ingredients in the *Astragalus-Coptis* drug pair and DKD targets, and the results were visualized using a Venn diagram. Additionally, gene expression levels in DKD were analyzed by retrieving samples from the Gene Expression Omnibus with "Diabetic Kidney Diseases" as the keyword and "*Homo sapiens*" as the organism. Gene expression data from DKD and normal kidney samples (GSE1009) were accessed[24]. The gene expression analysis data for GSE1009 were obtained from the GPL8300 platform (source: Affymetrix Human Gene Expression Panel). Thresholds of $|\log_2 FC| > 1$ and $P < 0.05$ were applied to identify DEGs[25]. Volcanoes and heatmaps were visualized using the ggplot2 and pheatmap packages in R software.

Construction of the "disease-active ingredient-target" network

The network was constructed using Cytoscape 3.10.1, with a focus on potential key objectives, followed by system analysis of the network parameters[26]. A network diagram of "disease-active ingredient-target" was generated using Cytoscape 3.10.1, incorporating the active ingredients of the *Astragalus-Coptis* drug pair and common and DKD targets. The topological properties of each node were calculated using the "CytoNCA" functional module in Cytoscape 3.10.1 to determine their significance, with nodes ranked based on degree value from high to low for core active ingredient identification.

Table 1 Databases and platform addresses

Database and platform	Address
TCMSP	http://www.tcmspw.com/tcmsp.php
Pubchem	https://pubchem.ncbi.nlmnih.gov
Novopro	https://www.novopro.cn/tools/mol2smiles.html
SwissADME	http://www.swissadme.ch
SwissTargetPrediction	http://www.swisstargetprediction.ch
GeneCards	https://www.genecards.org
OMIM	https://omim.org
DisGeNET	https://www.disgenet.org
VENNY2.1	http://bioinfogp.cnb.csic.es/tools/venny/
GEO	http://www.ncbi.nlm.nih.gov/geo/
STRING	https://string-db.org/
DAVID	https://david.ncifcrf.gov
Bioinformatics	https://www.bioinformatics.com.cn
BioGPS	https://biogps.org
RCSB	https://www.pdbus.org/

GEO: Gene Expression Omnibus; OMIM: Online Mendelian Inheritance in Man database.

Establishment of the protein-protein interaction network

The STRING database systematically compiles and integrates protein-protein interactions, encompassing physical contacts and functional associations[27]. Protein-protein interaction (PPI) analysis of common targets was conducted using the STRING database. Multiple proteins were selected, and *Homo sapiens* was chosen as the research subject to construct a PPI network diagram of common targets. The TSV file of the interaction network was exported. Cytoscape 3.10.1 was utilized to import the TSV files, and the CentiscaPe 2.2 function module was employed to calculate three network topology parameters: Degree centrality, betweenness centrality, and closeness centrality. Subsequently, the PPI network graph underwent optimization based on thresholds set for degree centrality, betweenness centrality, and closeness centrality values to identify key targets[28]. The MCODE plug-in in Cytoscape 3.10.1 was utilized to identify high-relevance modules in the PPI network based on topological parameters, including degree cutoff = 2, K-core = 2, node score cutoff = 0.2, and maximum depth = 100.

Gene Ontology enrichment analysis and Kyoto Encyclopedia of Genes and Genomes enrichment analysis

The joint utilization of the DAVID enrichment analysis platform is sought to enhance our understanding of the functional significance of common targets[29]. Gene Ontology (GO) biological function analysis and Kyoto Encyclopedia of Genes and Genomes (KEGG) pathway enrichment analysis were performed separately[30]. GO functional enrichment analysis included three categories: Biological process (BP), cellular component (CC), and molecular function (MF). The results of the enrichment analysis were exported, and based on the *P* value, the top 20 enriched terms in both GO and KEGG were closely examined for their relevance to DKD. A bioinformatics platform will be used for data visualization.

Construction of the "key target-organ" network

The precise mechanisms underlying the *in vivo* metabolism of the *Astragalus-Coptis* drug pair remain unclear, and multiple organs and tissues are likely involved in DKD treatment. To further investigate this possibility, microarray analysis was conducted using the BioGPS database to obtain the mRNA levels of key targets for each *Astragalus-Coptis* drug pair in various organ tissues[31]. Subsequently, a network map depicting the interconnectedness of these "key target-organ" was constructed using Cytoscape 3.10.1.

Construction of the "active ingredient-target-signaling pathway" network

To visualize and elucidate the intricate relationships among active ingredients, pathways, and targets, we imported the data on the core active ingredients of the *Astragalus-Coptis* drug pair, as well as the key targets and main pathways obtained through KEGG enrichment analysis, into Cytoscape 3.10.1 software for visualization purposes. Subsequently, a network diagram illustrating the "active ingredient-target-signaling pathway" was generated.

Molecular docking verification

The receptor of the *Astragalus-Coptis* drug pair was utilized as the key target for treating DKD, while its core active ingredient served as the ligand for molecular docking verification to analyze its binding affinity. The molecular structure data of the receptor and ligand proteins were obtained from the RCSB database and TCMSP database, respectively, and converted into pdb format. The receptor and ligand proteins were pretreated using PyMOL software to eliminate water molecules and the original ligands. AutoDock-Tools 1.5.6 software was used to conduct molecular docking between the processed receptors and ligand files, which were saved in "pdbqt" format. AutoDock Vina was used to calculate the minimum binding energy between each target and active ingredient, and a heatmap was generated on a bioinformatics platform for visualization purposes. Finally, PyMOL software was used to visualize the docking results.

MD simulation

Gromacs 2018 was chosen as the software for dynamics simulations, while OPLS was utilized for the force fields of both proteins and small molecules. The TIP3P water model was used to add water molecules to the system, with a 10 nm^3 × 10 nm^3 × 10 nm^3 water box established (ensuring that the edge of the water box was at least 1.2 nm away from the protein). An ion auto-balance system was also incorporated. Electrostatic interactions were handled using the particle-mesh Ewald method in conjunction with the steepest descent energy minimization (with a maximum of 50000 steps). The Coulomb force distance and van der Waals radius cutoff distances were set at 1 nm each. Subsequently, a canonical ensemble and an isothermal-isobaric ensemble were employed to equilibrate the system before conducting MD simulations for 100 ns under room temperature and pressure conditions. A nonbonded interaction cutoff value of 10 Ångstroms was applied. The V-rescale temperature coupling method maintained the simulation temperature at 300 K, while pressure control was achieved using the Berendsen method at 1 bar. Calculating binding free energy allows the assessment of intermolecular interaction strength within receptor-ligand complexes by quantifying contributions from various chemical energies. The Molecular Mechanics Poisson-Boltzmann Surface Area method provides a straightforward means to quantify the binding free energy between receptors and ligands[32]. The binding free energy was computed using the gmx_MMPBSA tool implemented in GROMACS[33].

RESULTS

Active ingredients and potential targets of the Astragalus-Coptis drug pair

The *Astragalus-Coptis* drug pair was selected from the TCMSP database, resulting in 135 active ingredients. To meet the criteria, these active ingredients had to have an OB equal to or greater than 30%, a DL value equal to or greater than 0.18, a "high" gastrointestinal absorption score according to the SwissADME platform, and at least two positive results for the five principles of drug similarity (Lipinski, Ghose, Veber, Egan, Muegge). After applying these criteria, we identified 27 active ingredients from the *Astragalus-Coptis* drug pair (Table 2). Subsequently, using the SwissTargetPrediction database for target prediction analysis of these 27 active ingredients resulted in 1646 predicted targets. After removing duplicates, we obtained a final list of 512 unique targets for these active ingredients.

DKD targets and common targets

The integration of 2961, 1818, and 1189 DKD targets obtained from the GeneCards, OMIM, and DisGeNET databases yielded 4044 unique DKD targets (Figure 1A). By employing the Venny 2.1 tool to compare the active ingredient targets with the DKD targets, a Venn diagram was generated (Figure 1B), revealing a set of 273 common targets. Furthermore, DEG between DKD samples and normal samples in the test group using GSE1009 data identified 34 upregulated genes and 16 downregulated genes (Table 3). Volcano plots and heatmaps illustrating the differential gene expression data for DKD are presented in Figure 1C and D.

"Disease-active ingredient-target" network

The DKD targets, the active ingredients of the *Astragalus-Coptis* drug pair, and the common targets were imported into Cytoscape 3.10.1 to generate a network diagram of "disease-active ingredient-target", as depicted in Figure 2, consisting of 303 nodes and 1253 edges. The degree value for each active ingredient was calculated using the "CytoNCA" functional module to determine their topological importance, resulting in a ranking from highest to lowest degree. Following network analysis, active ingredients with a degree ≥ 56 were selected. Among them, 3,9-di-O-methylnissolin, isorhamnetin, jaranol, quercetin, 1-7-dihydroxy-3,9-dime-thoxypterocarpene, (3R)-3-(2-hydroxy-3,4-dimethoxyphenyl)chroman-7-ol, palmatine, obacunone, and moupinamide were found to be associated with 66, 63, 63, 62, 62, 58, 57, and 56 disease targets, respectively, in this study. These active ingredients may serve as core ingredients in the *Astragalus-Coptis* drug pair for treating DKD (Table 4).

Construction and analysis of the protein-protein interaction network

To investigate the mechanism of action of the *Astragalus-Coptis* drug pair in treating DKD, we input 273 common targets associated with this drug pair into the STRING database for PPI analysis (Figure 3A). The resulting PPI network TSV file was imported into Cytoscape 3.10.1 software to construct a visual representation of the PPI network diagram, excluding nodes that had no interaction with other nodes. Consequently, we obtained a PPI network consisting of 271 nodes and 4129 edges (Figure 3B). Cluster analysis using MCODE was performed to generate a highly connected subnetwork and assign targets to four groups (Figure 3C). By utilizing the CentiscaPe 2.2 functional module, we determined thresholds for

Table 2 Active ingredients of the *Astragalus-Coptis* drug pair

TCM	Serial number	MOL ID	Ingredient	OB (%)	DL
Astragalus membranaceus	HQ1	MOL000379	9,10-dimethoxypterocarpan-3-O-β-D-glucoside	36.74	0.92
	HQ2	MOL000387	Bifendate	31.10	0.67
	HQ3	MOL000442	1,7-Dihydroxy-3,9-dimethoxy pterocarpene	39.05	0.48
	HQ4	MOL000371	3,9-di-O-methylnissolin	53.74	0.48
	HQ5	MOL000380	(6aR,11aR)-9,10-dimethoxy-6a,11a-dihydro-6H-benzofurano[3,2-c]chromen-3-ol	64.26	0.42
	HQ6	MOL000354	Isorhamnetin	49.60	0.31
	HQ7	MOL000378	7-O-methylisomucronulatol	74.69	0.30
	HQ8	MOL000398	Isoflavanone	109.99	0.03
	HQ9	MOL000239	Jaranol	50.83	0.29
	HQ10	MOL000098	Quercetin	46.43	0.28
	HQ11	MOL000438	(3R)-3-(2-hydroxy-3,4-dimethoxyphenyl)chroman-7-ol	67.67	0.26
	HQ12	MOL000417	Calycosin	47.75	0.24
	HQ13	MOL000422	Kaempferol	41.88	0.24
	HQ14	MOL000392	Formononetin	69.67	0.21
Coptis chinensis Franch	HL1	MOL002903	(R)-Canadine	55.37	0.77
	HL2	MOL001454	Berberine	36.86	0.78
	HL3	MOL002894	Berberrubine	35.74	0.73
	HL4	MOL002904	Berlambine	36.68	0.82
	HL5	MOL001458	Coptisine	30.67	0.86
	HL6	MOL002907	Corchoroside A_qt	104.95	0.78
	HL7	MOL002897	Epiberberine	43.09	0.78
	HL8	MOL000622	Magnograndiolide	63.71	0.19
	HL9	MOL008647	Moupinamide	86.71	0.26
	HL10	MOL013352	Obacunone	43.29	0.77
	HL11	MOL000785	Palmatine	64.60	0.65
	HL12	MOL000098	Quercetin	46.43	0.28
	HL13	MOL002668	Worenine	45.83	0.87

DL: Drug-likeness; MOL: Molecule; OB: Oral bioavailability; TCM: Traditional Chinese medicine.

DC (degree centrality), BC (betweenness centrality), and CC (closeness centrality) within the common target interaction network as follows: DC = 30.47232472, BC = 303.9409594, and CC = 0.001774064, respectively. Based on topological analysis using these thresholds as screening criteria, we identified a core PPI network comprising 10 key targets: AKT serine/threonine kinase 1 (AKT1) (degree value: 46), epidermal growth factor receptor (EGFR) (degree value: 44), tumor necrosis factor (TNF) (degree value: 43), SRC proto-oncogene, non-receptor tyrosine kinase (SRC) (degree value: 43), Jun proto-oncogene, AP-1 transcription factor subunit (JUN) (degree value: 43), caspase 3 (CASP3) (degree value: 43), mitogen-activated protein kinase 3 (MAPK3) (degree value: 43), heat shock protein 90 alpha family class A member 1 (HSP90AA1) (degree value: 41), signal transducer and activator of transcription 3 (STAT3) (degree value: 40), and estrogen receptor 1 (ESR1) (degree value: 38) (Figure 3D, Table 5). These targets may have significant implications for understanding the pathogenesis and treatment of DKD.

GO enrichment analysis

The 273 common targets of the *Astragalus-Coptis* drug pair in treating DKD were entered into the DAVID database for GO function and KEGG pathway enrichment analysis. A total of 1265 items were obtained through GO functional enrichment analysis, including 937 BP, 122 CC, and 206 MF terms. The respective items within each category were sorted based on their *P* values from smallest to largest, and the top 20 items were selected for visualization, as depicted in Figure 4. The results revealed that cell BP included protein phosphorylation, negative regulation of apoptotic process, and the inflammatory response. The primary CCs included mitochondrion, extracellular exosome, and membrane raft. The main MF

Table 3 Information on the differential gene expression analysis identified from the Gene Expression Omnibus dataset

Gene symbol	Protein name	Log_2FC	*P* value	Change
PLCE1	Phospholipase C epsilon 1	3.980421	0.00000765	Upregulated
CLIC5	Chloride intracellular channel 5	4.380969	0.00001522	Upregulated
PTPRO	Protein tyrosine phosphatase receptor type O	3.922249	0.00001810	Upregulated
HSPA12A	Heat shock protein family A (Hsp70) member 12A	4.194141	0.00001836	Upregulated
AIF1	Allograft inflammatory Factor 1	3.616273	0.00002007	Upregulated
GMDS	GDP-mannose 4,6-dehydratase	3.900218	0.00002555	Upregulated
SEMA5A	Semaphorin 5A	3.956868	0.00002673	Upregulated
CEP152	Centrosomal protein 152	4.004339	0.00002683	Downregulated
FOXC1	Forkhead Box C1	3.505715	0.00003095	Upregulated
MME	Membrane metalloendopeptidase	3.837958	0.00003666	Upregulated
FGF1	Fibroblast growth Factor 1	3.743398	0.00003695	Upregulated
TNNC1	Troponin C1, slow skeletal and cardiac type	3.602037	0.00004852	Upregulated
CYP2C8	Cytochrome P450 family 2 subfamily C member 8	-3.55671	0.00004895	Downregulated
THBS1	Thrombospondin 1	3.170090	0.00005034	Upregulated
VEGFA	Vascular endothelial growth Factor A	4.261645	0.00005391	Upregulated
LUNAR1	Leukemia-associated noncoding IGF1R activator RNA 1	3.265115	0.00005733	Downregulated
HOXD1	Homeobox D1	3.812893	0.00005999	Upregulated
BMP2	bone morphogenetic protein 2	3.115485	0.00006297	Upregulated
IQGAP2	IQ motif containing GTPase activating protein 2	2.540433	0.00006536	Upregulated
ST3GAL6	ST3 beta-galactoside alpha-2,3-sialyltransferase 6	2.858100	0.00006870	Upregulated
THSD7A	Thrombospondin type 1 domain containing 7A	2.581030	0.00006966	Upregulated
F2R	Coagulation factor II thrombin receptor	2.809148	0.00007121	Upregulated
SLC9A1	Solute carrier family 9 member A1	4.330925	0.00007424	Downregulated
ADORA2B	Adenosine A2b receptor	2.582378	0.00008127	Downregulated
FAM153A	Family with sequence similarity 153 member A	3.774375	0.00009200	Upregulated
ITGB1	Integrin subunit beta 1	3.774328	0.00009284	Downregulated
CDS1	CDP-diacylglycerol synthase 1	2.695287	0.00009577	Upregulated
EGR2	Early growth response 2	3.580285	0.00010401	Downregulated
PLA2R1	Phospholipase A2 receptor 1	3.485108	0.00010718	Upregulated
GAS1	Growth arrest specific 1	3.659052	0.00010882	Upregulated
TYRO3	TYRO3 protein tyrosine kinase	2.854082	0.00011003	Upregulated
LOC101929500	Uncharacterized LOC101929500	2.664931	0.00011229	Upregulated
F3	Coagulation factor III, tissue factor	3.035691	0.00011752	Upregulated
XPNPEP2	X-prolyl aminopeptidase 2	3.454828	0.00013038	Downregulated
FUT6	Fucosyltransferase 6	3.357247	0.00013492	Downregulated
LCN1	Lipocalin 1	2.654097	0.00014868	Downregulated
C1orf21	Chromosome 1 open reading frame 21	2.655885	0.00015593	Upregulated
LOC103344931	Uncharacterized LOC103344931	2.423861	0.00015641	Upregulated
FRY	FRY microtubule binding protein	2.922064	0.00016127	Upregulated
POU2F2	POU class 2 homeobox 2	-2.51972	0.00016162	Downregulated
VEGFA	Vascular endothelial growth Factor A	2.860180	0.00016446	Upregulated

CHRNE	Cholinergic receptor nicotinic epsilon subunit	2.954435	0.00016654	Downregulated
TUBB4A	Tubulin beta 4A class IVa	3.908527	0.00016713	Downregulated
MGAT5	Alpha-1,6-mannosylglycoprotein 6-beta-N-acetylglucosaminyltransferase	2.568678	0.00017864	Upregulated
PTPRD	Protein tyrosine phosphatase receptor type D	3.052249	0.00018095	Upregulated
HYAL1	Hyaluronidase 1	-2.217640	0.00018409	Downregulated
DPYSL3	Dihydropyrimidinase like 3	3.782204	0.00018554	Upregulated
UGT2B17	UDP glucuronosyltransferase family 2 member B17	2.604504	0.00018633	Downregulated
PAM	Peptidylglycine alpha-amidating monooxygenase	2.25575	0.00018848	Upregulated
RFC4	Replication Factor C subunit 4	3.094109	0.00020080	Downregulated

Table 4 Core active ingredients of the *Astragalus-Coptis* drug pair

Serial number	MOL ID	Ingredient	Degree
HQ4	MOL000371	3,9-di-O-methylnissolin	66.0
HQ6	MOL000354	Isorhamnetin	63.0
HQ9	MOL000239	Jaranol	63.0
HQ10, HL12	MOL000098	Quercetin	62.0
HQ13	MOL000422	1,7-Dihydroxy-3,9-dimethoxy pterocarpene	62.0
HQ11	MOL000438	(3R)-3-(2-hydroxy-3,4-dimethoxyphenyl)chroman-7-ol	58.0
HL11	MOL000785	Palmatine	58.0
HL10	MOL013352	Obacunone	57.0
HL9	MOL008647	Moupinamide	56.0

Table 5 Analysis of topological parameters of key targets

Name	Degree centrality	Betweenness centrality	Closeness centrality	Degree
AKT1	155	6135.22026848002	0.00258397932816537	46
EGFR	127	2630.66165751648	0.00239234449760765	44
TNF	155	6936.3437260436	0.00257069408740359	43
SRC	129	3308.84927642964	0.00240384615384615	43
JUN	117	1696.42973120389	0.00232018561484918	43
CASP3	116	2086.85812276904	0.00233644859813084	43
MAPK3	119	2232.21929446136	0.00233100233100233	43
HSP90AA1	124	3622.00791458381	0.00235849056603773	41
STAT3	123	1881.06728458254	0.00234192037470726	40
ESR1	102	1938.43441498511	0.00224215246636771	38

were protein serine/threonine/tyrosine kinase activity, ATP binding, and protein kinase activity.

KEGG enrichment analysis

KEGG pathway enrichment analysis identified 185 related pathways, which were then ranked by *P* value from smallest to largest. The top 20 pathways were selected for further analysis (Figure 5A and B; Table 6). The core active ingredients of the *Astragalus-Coptis* drug pair in the treatment of DKD, along with common targets and the top 20 KEGG signaling pathways, were imported into Cytoscape 3.10.1 software to construct a comprehensive active ingredient-target-signaling pathway network diagram (Figure 5C). This network graph consisted of a total of 80 nodes and 385 edges. The results demonstrated that the *Astragalus-Coptis* drug pair has synergistic effects on treating DKD through multiple ingredients, targets, and pathways. The *P* value for the advanced glycation end products (AGE)-receptor for AGEs (AGE-RAGE) signaling pathway in diabetic complications was 2.05E-22, while the gene number was 31. In addition, 40 genes related to

Table 6 Kyoto Encyclopedia of Genes and Genomes enrichment results

ID	Term	Enrichment	*P* value	Count
hsa04933	AGE-RAGE signaling pathway in diabetic complications	10.2107004	2.05E-22	31
hsa05417	Lipid and atherosclerosis	6.12795222	3.17E-20	40
hsa04151	PI3K-Akt signaling pathway	4.55917914	3.19E-19	49
hsa04066	HIF-1 signaling pathway	8.15889052	7.92E-17	27
hsa04510	Focal adhesion	5.67892124	1.28E-16	35
hsa04014	Ras signaling pathway	5.16396821	4.42E-16	37
hsa04012	ErbB signaling pathway	8.91256580	3.47E-15	23
hsa04664	Fc epsilon RI signaling pathway	10.1719501	4.44E-15	21
hsa04931	Insulin resistance	7.62447759	7.90E-15	25
hsa04068	FoxO signaling pathway	6.78869516	1.03E-14	27
hsa04010	MAPK signaling pathway	4.25354962	3.49E-14	39
hsa04062	Chemokine signaling pathway	5.31807312	7.06E-14	31
hsa04926	Relaxin signaling pathway	6.38328356	5.15E-13	25
hsa05418	Fluid shear stress and atherosclerosis	5.92405453	2.81E-12	25
hsa04668	TNF signaling pathway	6.64533415	2.32E-12	23
hsa04657	IL-17 signaling pathway	5.95682590	1.70E-08	17
hsa04922	Glucagon signaling pathway	4.30961126	1.88E-05	14
hsa04614	Renin-angiotensin system	10.0245305	4.72E-05	7
hsa04960	Aldosterone-regulated sodium reabsorption	7.12167420	1.01E-04	8
hsa04152	AMPK signaling pathway	4.89982957	1.15E-07	18

the Lipid and atherosclerosis pathway had a *P* value of 3.17E-20. The *Astragalus-Coptis* drug pair may play crucial roles in DKD treatment through these two core pathways. Based on the analysis of the differentially expressed genes mentioned above, we reconstructed a KEGG pathway map for the core pathway (Figure 6) and constructed a Sankey diagram using a bioinformatics platform to illustrate the relationships between the targets and pathways (Figure 5D).

Analysis of the "key target-organ network"

We analyzed the mRNA distribution levels across various cells, organs, and tissues for the 10 key targets. Notably, there was a significant increase in the mRNA levels of genes related to 23 specific entities, including the kidney, adrenal gland, adrenal cortex, prostate, thyroid gland, liver, cardiomyocytes, CD4+ T cells, CD8+ T cells and others. To demonstrate the associations between these key targets and organ tissues mentioned above, we constructed a "key target-organ network" consisting of 33 nodes and 130 edges (Figure 7). Network analysis revealed that these organs were primarily closely linked with the kidney and immune-related factors such as CD34+ T cells, CD4+ T cells, and CD8+ T cells. This finding suggested that the *Astragalus-Coptis* drug pair may exert therapeutic effects on DKD by activating renal function and systemic immunity.

Molecular docking

The ligands were selected based on the highest degree value in the "disease-active ingredient-target" network analysis, which included 9 core active ingredients. Molecular docking was then performed with the key target receptors AKT1, EGFR, TNF, SRC, JUN, CASP3, MAPK3, HSP90AA1, STAT3, and ESR1. AutoDock software was used to calculate the minimum binding energy, and the results are presented in Figure 8 as a heatmap. A lower binding energy indicates a stronger binding capacity between the ligand and receptor. Specifically, a binding energy ≤ -5.0 kcal/mol suggests moderate binding capacity, while a binding energy ≤ -7.0 kcal/mol indicates high binding capacity[34]. The binding energies of quercetin and obacunone to the key target were below -6.0 kcal/mol, while the binding energies of the other ingredients to the target were mostly lower than -5.0 kcal/mol. This indicates that the *Astragalus-Coptis* drug pair exhibits strong binding affinity for both the core active ingredients and the key targets, particularly between quercetin, obacunone, and the targets. The ingredient-target interactions with the smallest fraction of binding energy and their corresponding binding modes were visualized using PyMOL 1.7.2.1 and Discovery Studio 2020 (Figure 9). Notably, quercetin displayed the lowest binding energy with the TNF target (-9.95 kcal/mol), which can be attributed to its interaction with GLN-B:27 through hydrogen bonds formed with residues LEU-B:26 and ILE-B:136, a C-H bond formed with residue GLU-B:135, and a hydrophobic interaction involving residue PRO-B:139 of TNF (Figure 9J).

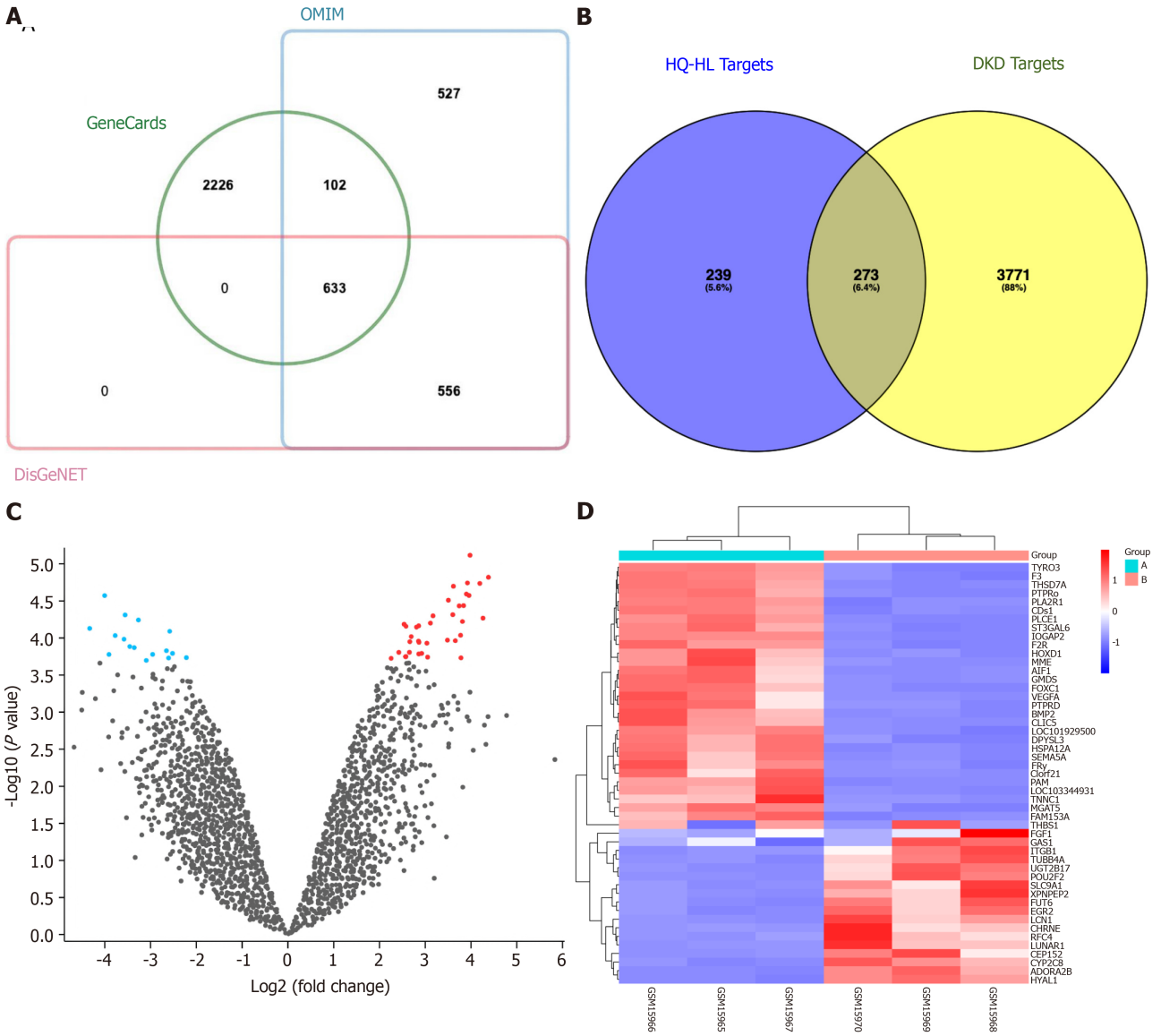

Figure 1 Screening of *Astragalus-Coptis* drug pair common targets. A: Venn diagram illustrating the target genes associated with diabetic kidney disease (DKD); B: Venn diagram depicting the 273 common targets between the active ingredient targets and DKD targets; C: Volcano plot displaying differential gene expression patterns in DKD samples, where red and blue indicate upregulated and downregulated genes, respectively, while gray represents no significant difference; D: Heatmap presenting the expression profiles of these 50 differential gene expression analysis. Columns correspond to sample groups, while rows represent individual genes. The cyan Group A denotes normal samples, whereas the red Group B signifies DKD samples. OMIM: Online Mendelian Inheritance in Man database.

MD simulation and binding free energy

MD simulation is a crucial method for investigating the stability and dynamics of protein complexes in aqueous solutions. To validate the binding stability of the ligand-receptor protein complex, MD simulations were conducted for 100 ns based on the results obtained from molecular docking studies involving the HL10 (obacunone)-MAPK3, HQ10 (quercetin)-AKT1, and HQ10 (quercetin)-TNF protein complexes.

The atomic root mean square deviation (RMSD) serves as a reliable metric for assessing the conformational stability of both the receptor and ligand while also quantifying the degree to which atomic positions deviate from their initial state. Lower deviations indicate enhanced conformational stability[35]. The Rg value can reflect the compactness of the binding structure and the degree of constraint of the system. Low Rg values indicate dense and compact systems[36]. The system stability can be assessed by measuring the RMSD and Rg. Based on the corresponding RMSD and Rg values for the three protein complexes (Figure 10A and B), it is evident that during the 100 ns MD simulation, the protein complexes exhibited a predominantly stable state with no significant structural alterations.

The root mean square fluctuation (RMSF) can effectively capture the volatility and flexibility of amino acid sites, as demonstrated in Figure 10C. Notably, the RMSF values for all residues within the three systems were consistently below 0.5 nm, except the first terminal residue. This observation strongly suggested that the core structure of the three-protein complex exhibited remarkable rigidity.

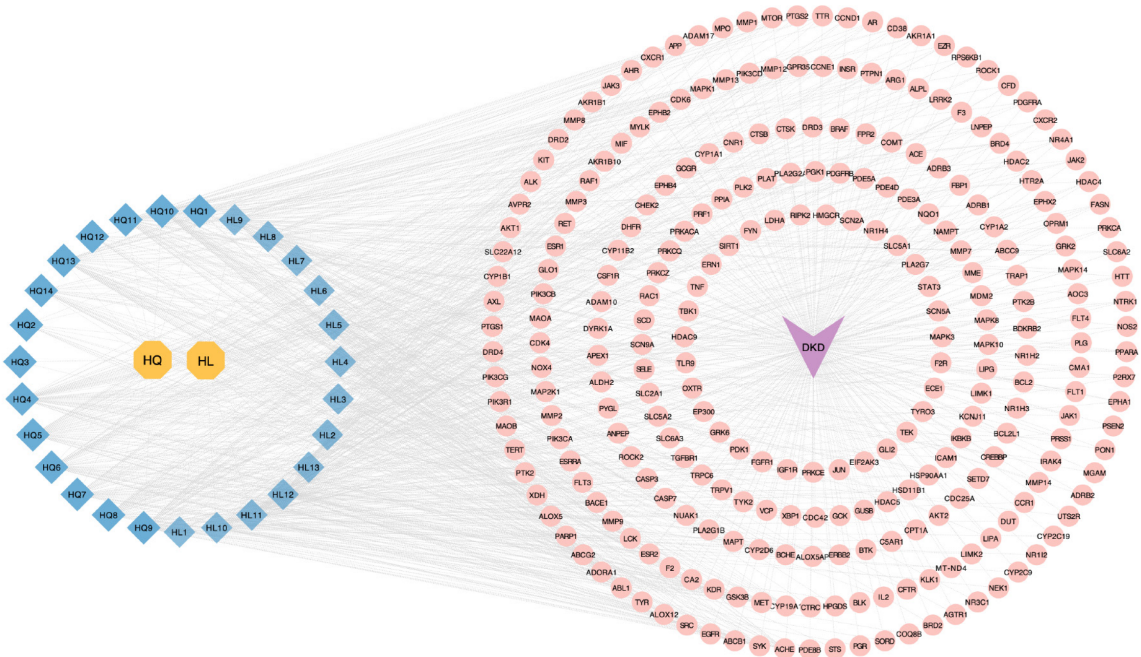

Figure 2 Disease-active ingredient-target network. The yellow octagon nodes represent the *Astragalus-Coptis* drug pair, while the blue prismatic nodes depict the active ingredients in this drug pair. The purple arrow nodes symbolize diabetic kidney disease, and the pink circular nodes represent the common targets. The edges illustrate the interaction between the active ingredient and its target. DKD: Diabetic kidney disease.

Hydrogen bonding is one of the most robust noncovalent binding interactions between an acceptor and a ligand, and a greater number of hydrogen bonds contributes to enhanced binding stability. Analysis of hydrogen bonds (Figure 10D) revealed that in the HQ10-AKT1 system, most time scales exhibited 1 to 3 hydrogen bonds, with a maximum of 4 hydrogen bonds observed. In the HQ10-TNF system, there was a significant increase in frames with a high number of hydrogen bonds (≥ 3), reaching a maximum of 5 hydrogen bonds. Conversely, only one hydrogen bond was present in the HL10-MAPK3 system. The formation of hydrogen bonds between the ligand and receptor plays a crucial role in stabilizing the protein-protein complex.

The overall secondary structure diagram of the protein complex (Supplementary Figure 1) revealed no significant fluctuations in the secondary structures, such as B-sheet, B-bridge, or bend structures, during the 100 ns MD simulation. The solvent-accessible surface area represents the degree of exposure of the protein surface. The results indicated that MAPK3 exhibited greater effects than did AKT1 and TNF. Both TNF and MAPK3 proteins displayed comparable exposure to hydrophobic and hydrophilic surfaces, while AKT1 had a slightly larger hydrophilic surface than a hydrophobic surface.

In parallel, we analyzed the binding free energy between the HL10 (obacunone)-MAPK3, HQ10 (quercetin)-AKT1, and HQ10 (quercetin)-TNF protein complexes. The GGAS parameter represents the free energy of the gas phase, which is determined through a comprehensive calculation involving van der Waals energy (VDWAALS) and electrostatic energy (EEL). Additionally, the nonpolar solvation energy (ESURF), although its value is negligible, and the polar solvation energy (EGB) in GSOLV were examined to assess the influence of polar solvents on binding affinity. These findings are illustrated in Figure 11.

The mean VDWAALS and mean EEL values were negative for the HQ10-AKT1, HQ10-TNF, and HL10-MAPK3 complexes (-12.75 kcal/mol and -0.77 kcal/mol; -14.65 kcal/mol and -10.13 kcal/mol; -1.32 kcal/mol and -0.30 kcal/mol, respectively), indicating a favorable combination of van der Waals energy and EEL in these complexes. However, the average EGB in GSOLV was relatively positive (7.60 kcal/mol, 16.15 kcal/mol and 1.05 kcal/mol, respectively). Although the average ESURF was negative (-1.52 kcal/mol, -1.97 kcal/mol, and -0.18 kcal/mol, respectively), the overall average GSOLV values were positive (6.08 kcal/mol, 14.18 kcal/mol, and 0.87 kcal/mol, respectively), suggesting that polar solvents are unfavorable for binding interactions. The average binding free energies were -7.44 kcal/mol ± 6.35 kcal/mol, -10.60 kcal/mol ± 9.98 kcal/mol, and -0.75 kcal/mol ± 2.97 kcal/mol, respectively. From these results, it can be concluded that all three protein complexes are stable. However, the HQ10-TNF protein complex exhibits stronger binding stability due to its greater content of van der Waals forces and hydrogen bonds.

After conducting MD simulations, we observed alterations in the interaction forces between ligands and receptors within all protein complexes of HQ10-AKT1, HQ10-TNF, and HL10-MAPK3 (Supplementary Figure 2). The combination of HQ10 and AKT1 in Supplementary Figure 2B is stabilized by two conventional hydrogen bonds with LEU347 and GLU341, one carbon-hydrogen bond and a conventional hydrogen bond with ARG346, as well as a Pi-Pi stacking interaction with TYR350. Additionally, van der Waals forces contribute to stabilizing its binding complex through interactions with ARG243, GLY345, and LEU239. The interaction between HQ10 and TNF in Supplementary Figure 2D is mediated by two hydrogen bonds with GLN27 and ASN19, one hydrogen bond with ILE136, one carbon-hydrogen bond with GLU135, and a conventional hydrogen bond. Additionally, there is an alkyl interaction involving LEU26 and

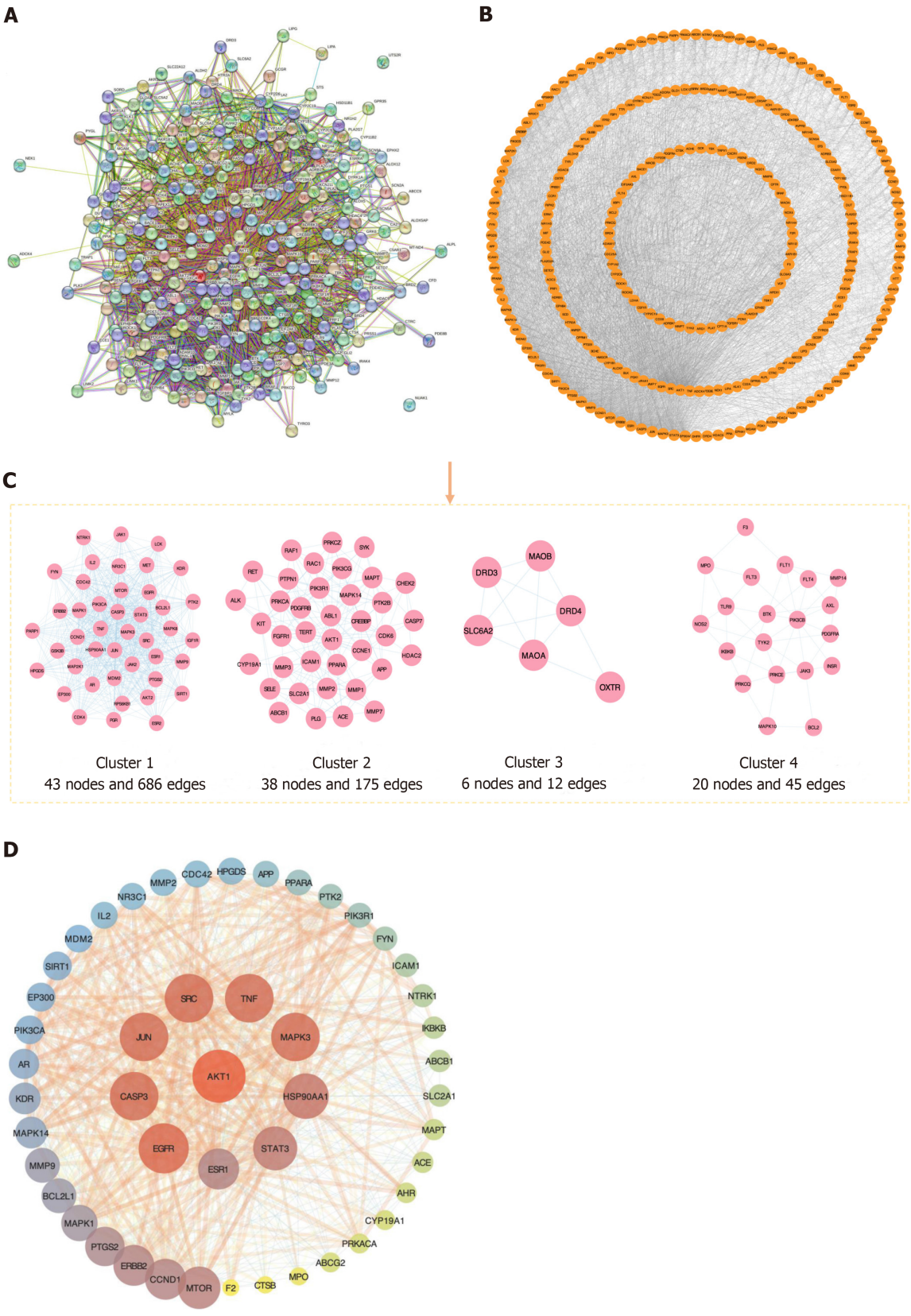

Figure 3 Protein-protein interaction network. A: The protein-protein interaction (PPI) network of common targets; B: The PPI network, commonly targeted, was optimized using Cytoscape 3.10.1; C: Cluster analysis-based construction of a PPI network utilizing MCODE plugin; D: The central core PPI network consisted of 48 nodes and 707 edges, wherein 10 nodes exhibiting an orange-to-purple gradient symbolized key targets associated with *Astragalus-Coptis* drug pair combination for treating diabetic kidney disease. Node sizes were proportionate to target degrees in the network.

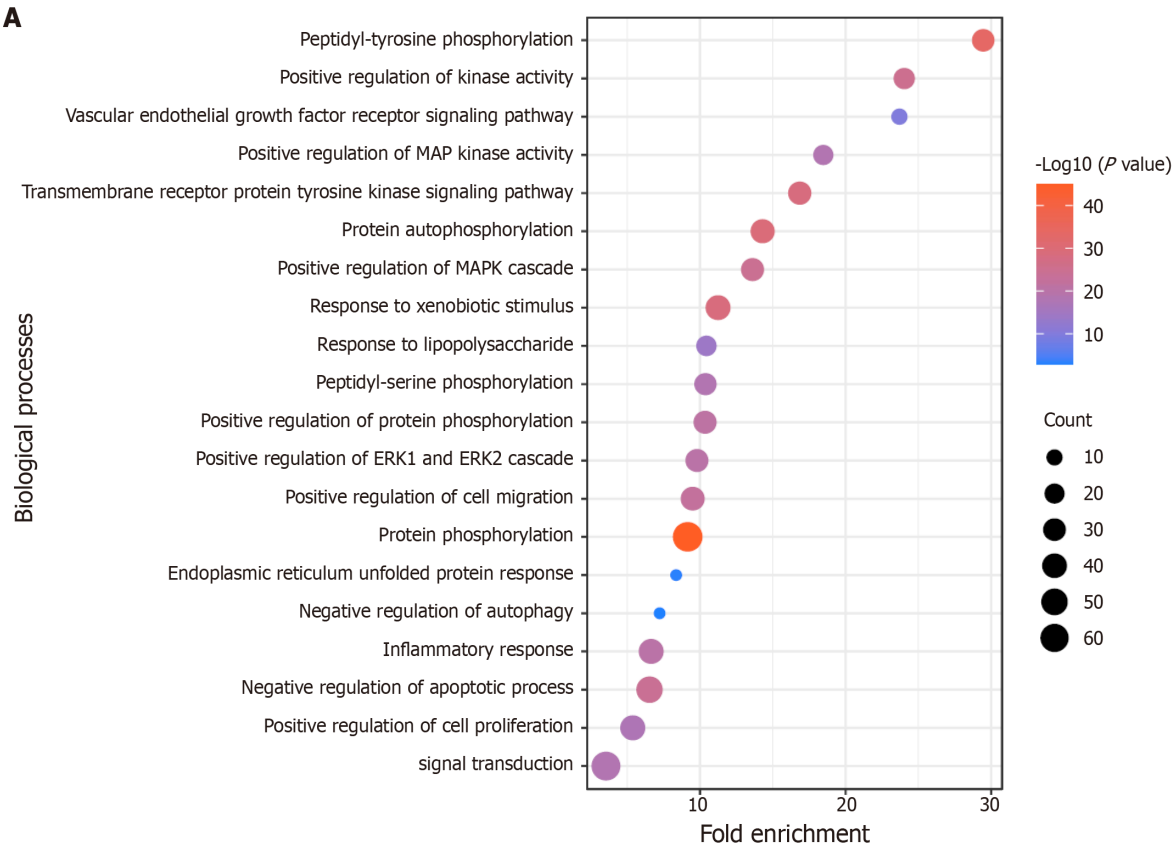
A
Peptidyl-tyrosine phosphorylation
Positive regulation of kinase activity
Vascular endothelial growth factor receptor signaling pathway
Positive regulation of MAP kinase activity
Transmembrane receptor protein tyrosine kinase signaling pathway
Protein autophosphorylation
Positive regulation of MAPK cascade
Response to xenobiotic stimulus
Response to lipopolysaccharide
Peptidyl-serine phosphorylation
Positive regulation of protein phosphorylation
Positive regulation of ERK1 and ERK2 cascade
Positive regulation of cell migration
Protein phosphorylation
Endoplasmic reticulum unfolded protein response
Negative regulation of autophagy
Inflammatory response
Negative regulation of apoptotic process
Positive regulation of cell proliferation
signal transduction
Biological processes
10
20
30
Fold enrichment
-Log10 (P value)
40
30
20
10
Count
10
20
30
40
50
60

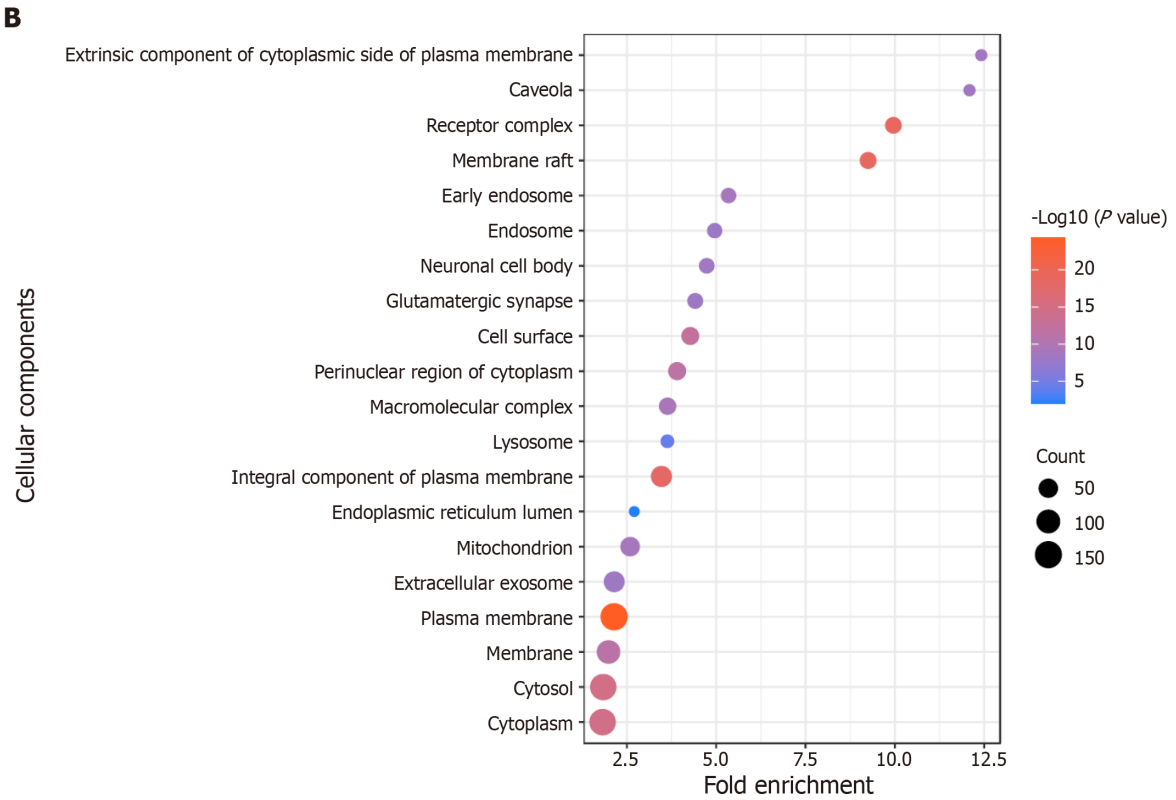
B
Extrinsic component of cytoplasmic side of plasma membrane
Caveola
Receptor complex
Membrane raft
Early endosome
Endosome
Neuronal cell body
Glutamatergic synapse
Cell surface
Perinuclear region of cytoplasm
Macromolecular complex
Lysosome
Integral component of plasma membrane
Endoplasmic reticulum lumen
Mitochondrion
Extracellular exosome
Plasma membrane
Membrane
Cytosol
Cytoplasm
Cellular components
2.5
5.0
7.5
10.0
12.5
Fold enrichment
-Log10 (P value)
20
15
10
5
Count
50
100
150

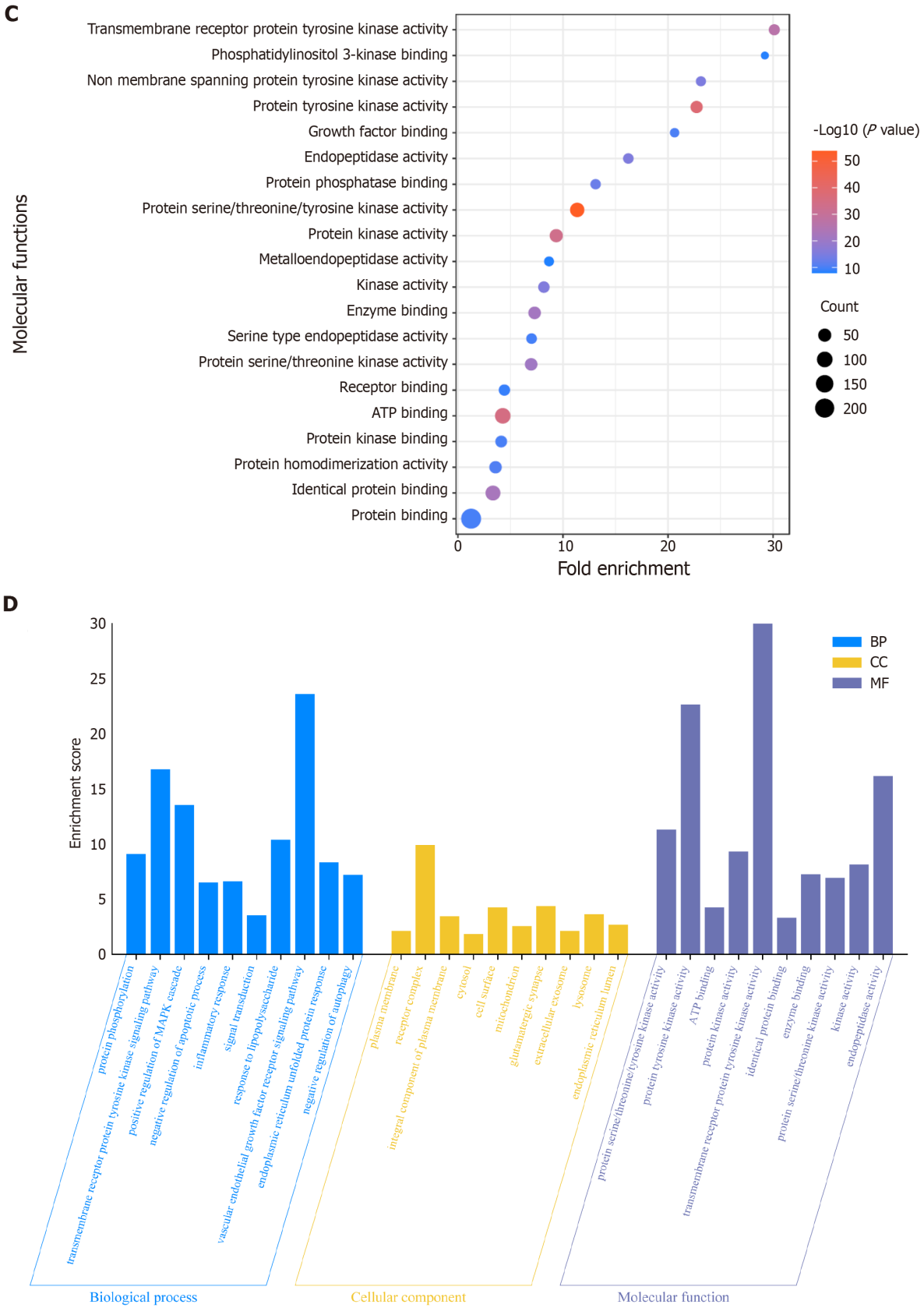

Figure 4 Gene Ontology enrichment diagram. A: Bubble map illustrating cellular biological processes (BP); B: Bubble plot depicting cellular components (CC); C: Bubble plot representing molecular function (MF). The X- and Y-axes display the fold enrichment and full name, respectively, while the color and size of the bubbles indicate the *P* value and number of genes, correspondingly; D: Top 10 BP, CC, and MF from Gene Ontology enrichment analysis are visualized as blue, orange, and purple bars, respectively.

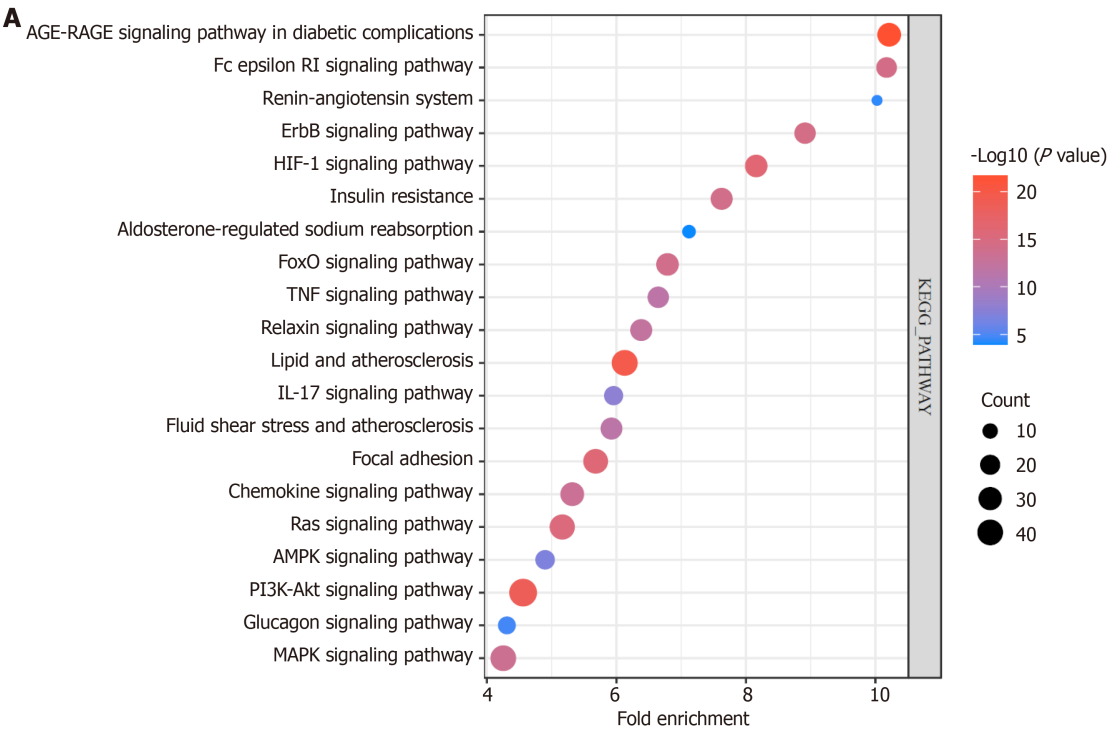
A
AGE-RAGE signaling pathway in diabetic complications
Fc epsilon RI signaling pathway
Renin-angiotensin system
ErbB signaling pathway
HIF-1 signaling pathway
Insulin resistance
Aldosterone-regulated sodium reabsorption
FoxO signaling pathway
TNF signaling pathway
Relaxin signaling pathway
Lipid and atherosclerosis
IL-17 signaling pathway
Fluid shear stress and atherosclerosis
Focal adhesion
Chemokine signaling pathway
Ras signaling pathway
AMPK signaling pathway
PI3K-Akt signaling pathway
Glucagon signaling pathway
MAPK signaling pathway
KEGG_PATHWAY
4
6
8
10
Fold enrichment
-Log10 (P value)
20
15
10
5
Count
10
20
30
40

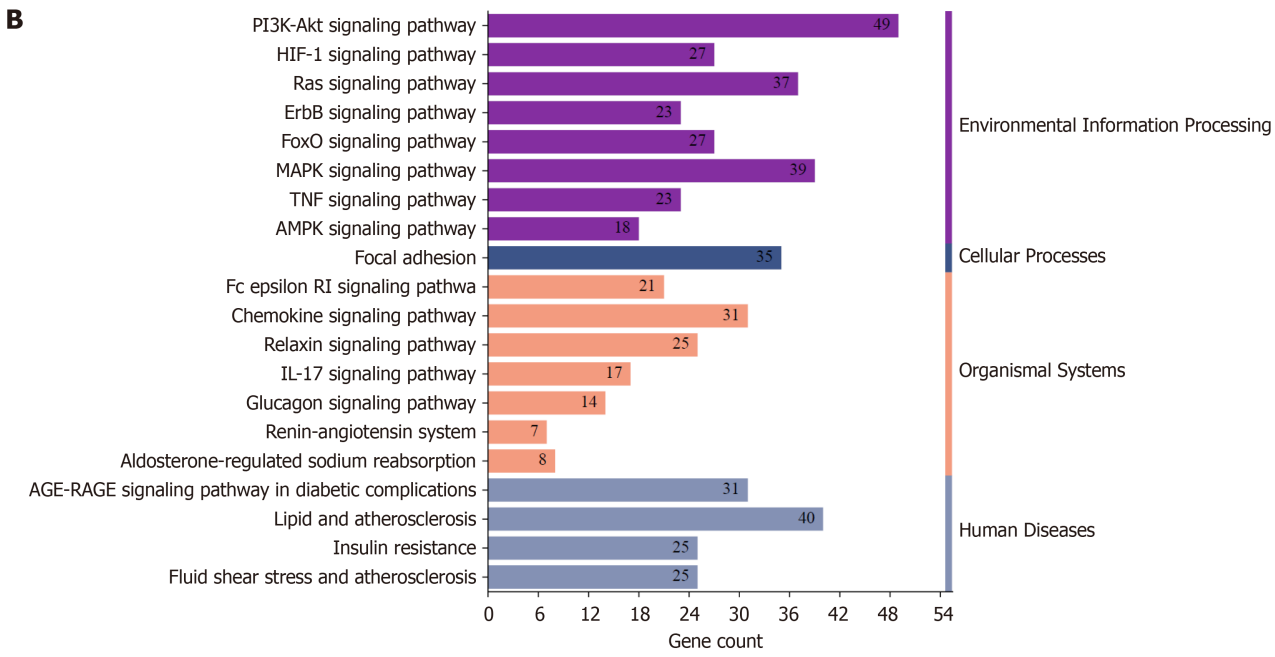
B
PI3K-Akt signaling pathway 49
HIF-1 signaling pathway 27
Ras signaling pathway 37
ErbB signaling pathway 23
FoxO signaling pathway 27
MAPK signaling pathway 39
TNF signaling pathway 23
AMPK signaling pathway 18
Focal adhesion 35
Fc epsilon RI signaling pathwa 21
Chemokine signaling pathway 31
Relaxin signaling pathway 25
IL-17 signaling pathway 17
Glucagon signaling pathway 14
Renin-angiotensin system 7
Aldosterone-regulated sodium reabsorption 8
AGE-RAGE signaling pathway in diabetic complications 31
Lipid and atherosclerosis 40
Insulin resistance 25
Fluid shear stress and atherosclerosis 25
0 6 12 18 24 30 36 42 48 54
Gene count
Environmental Information Processing
Cellular Processes
Organismal Systems
Human Diseases

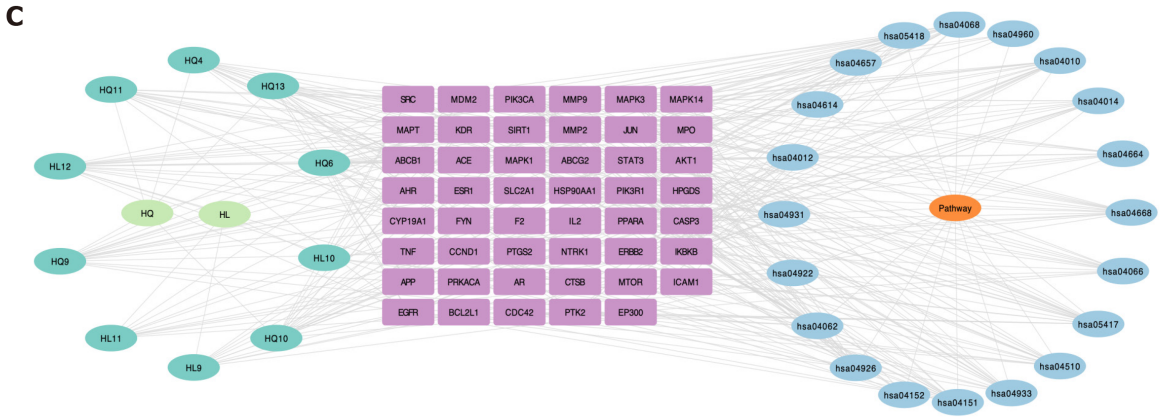
C
HQ4
HQ11
HQ13
HL12
HQ6
HQ
HL
HQ9
HL10
HL11
HQ10
HL9
SRC MDM2 PIK3CA MMP9 MAPK3 MAPK14
MAPT KDR SIRT1 MMP2 JUN MPO
ABCB1 ACE MAPK1 ABCG2 STAT3 AKT1
AHR ESR1 SLC2A1 HSP90AA1 PIK3R1 HPGDS
CYP19A1 FYN F2 IL2 PPARA CASP3
TNF CCND1 PTGS2 NTRK1 ERBB2 IKBKB
APP PRKACA AR CTSB MTOR ICAM1
EGFR BCL2L1 CDC42 PTK2 EP300
hsa05418
hsa04068
hsa04960
hsa04657
hsa04010
hsa04614
hsa04014
hsa04012
hsa04664
hsa04931
Pathway
hsa04668
hsa04922
hsa04066
hsa04062
hsa05417
hsa04926
hsa04510
hsa04152
hsa04151
hsa04933

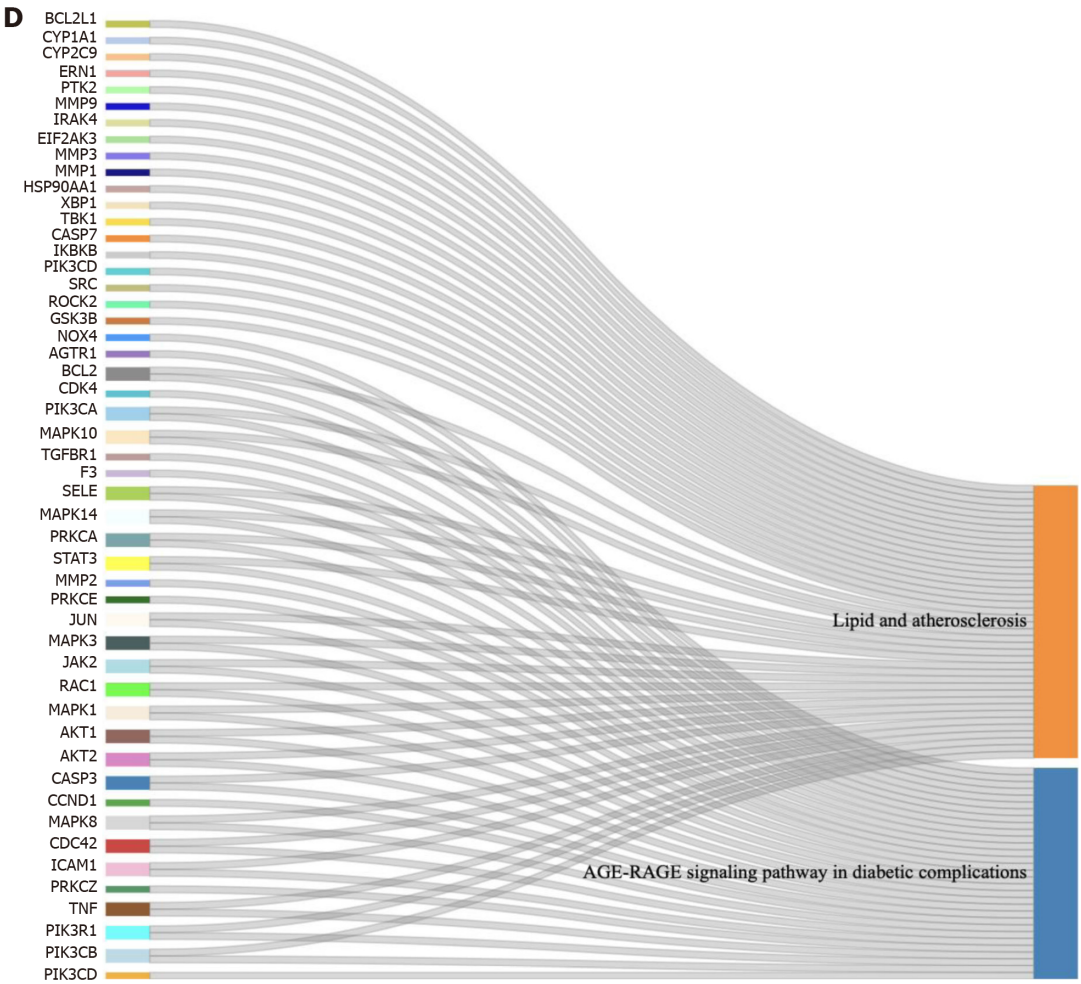

Figure 5 Kyoto Encyclopedia of Genes and Genomes pathway enrichment diagram. A: Bubble plot depicting the top 20 pathways identified through Kyoto Encyclopedia of Genes and Genomes (KEGG) enrichment analysis; B: Classification of the top 20 pathways based on KEGG enrichment analysis according to their respective KEGG types; C: Diagram illustrating the active ingredient-target-signaling pathway. The cyan node represents the active ingredient, while the purple node signifies the target. The blue node denotes the pathway itself; D: Sankey diagram showcasing KEGG core pathways. The left rectangular node in this sankey plot represents the target, whereas the right rectangular node symbolizes the corresponding KEGG pathway. The lines represent associations between targets and pathways.

PRO129. A pi-alkyl interaction occurs between LEU26 and ALA, which is stabilized through van der Waals forces from ASN46, VAL150, TRP28, ARG138, ASN137, LEU142, ALA22, and GLN21. The interaction between HL10 and MAPK in Supplementary Figure 2F is reinforced by a hydrogen bond and a carbon-hydrogen bond with ARG64, as well as the van der Waals forces contributed by LYS65 and THR66.

DISCUSSION

The therapeutic potential of the *Astragalus-Coptis* drug pair for DKD treatment has been supported by clinical and experimental studies. However, the active ingredients of the *Astragalus-Coptis* drug pair and the underlying mechanisms responsible for its therapeutic effects on DKD remain unclear. Therefore, we employed NP approaches, molecular docking, and MD simulations to elucidate the active ingredients, potential targets, and mechanisms of action associated with the *Astragalus-Coptis* drug pair in DKD.

According to the "disease-active ingredient-target" network topology analysis, the *Astragalus-Coptis* drug pair used to improve the core of DKD active ingredients include 3,9-di-O-methylnissolin, isorhamnetin, jaranol, quercetin, 1,7-dihydroxy-3,9-dimethoxy pterocarpene, (3R)-3-(2-hydroxy-3,4-dimethoxyphenyl)chroman-7-ol, palmatine, obacunone, and moupinamide. Relevant studies support the therapeutic effects of these active ingredients on DKD. Both quercetin and isorhamnetin mitigate the impact of DKD on renal function through their ability to lower glucose levels, enhance oxidative status, alleviate inflammation, and regulate lipid metabolism and adipocyte differentiation[37,38]. Additionally, quercetin can regulate renal lipid accumulation to prevent and alleviate DKD while also improving diabetic kidney injury through the Nrf2/HO-1 signaling pathway activation, which inhibits deiron[39,40]. Palmatine is a potent inhibitor of lipase that effectively reduces serum cholesterol and blood glucose levels. Furthermore, it exhibits a direct and/or indirect association with DKD[41]. Obacunone can alleviate high glucose-induced oxidative damage in NRK-52E cells by

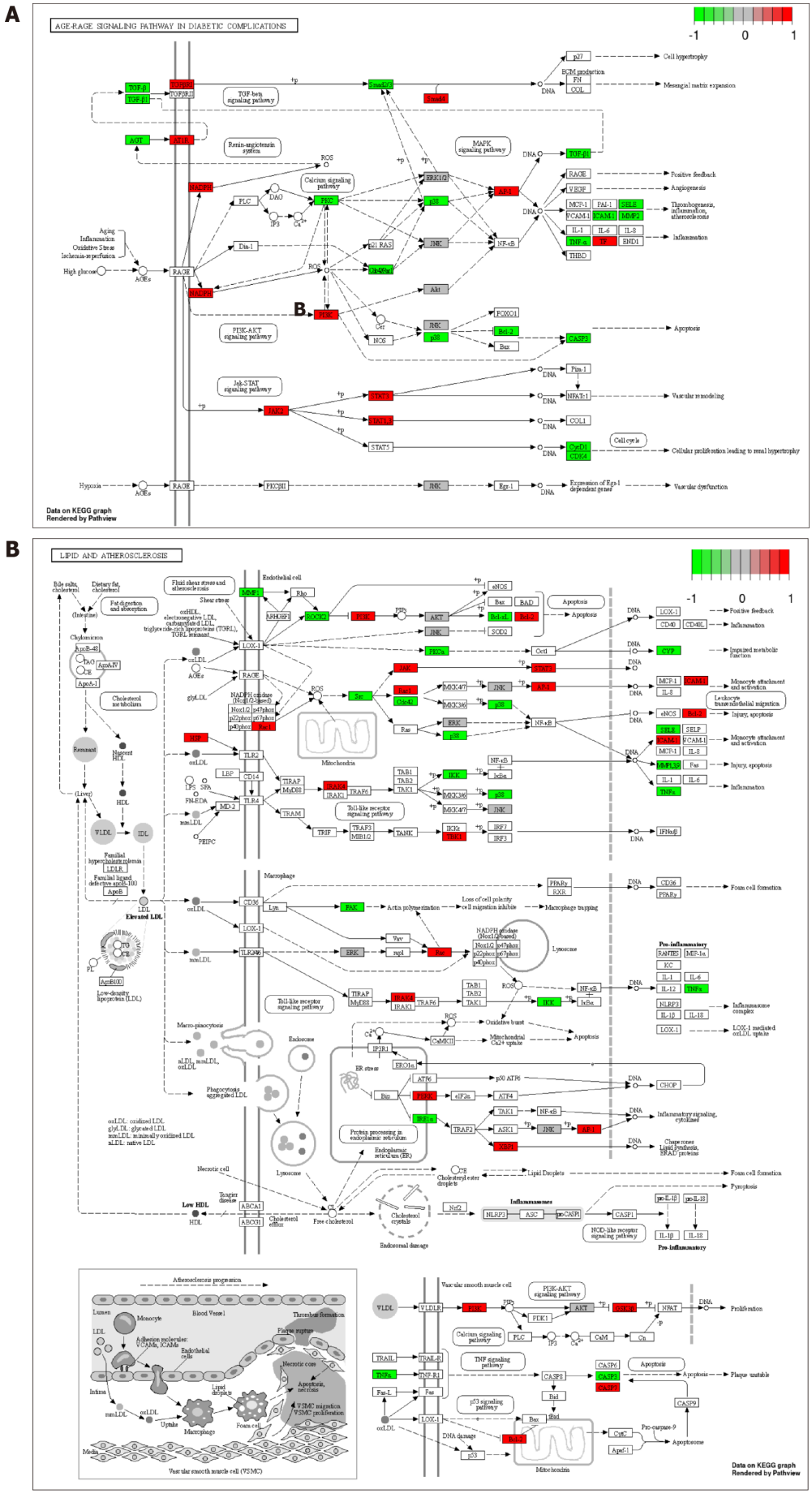

Figure 6 Distribution of common targets in the core pathways. A: Distribution of common targets associated with the advanced glycation end products

(AGE)-receptor for AGEs signaling pathway in diabetic complications; B: Distribution of relevant common targets in the Lipid and atherosclerosis pathway. Red, green, and gray rectangles represent upregulated and downregulated gene targets, respectively, without any significantly differentially expressed gene targets.

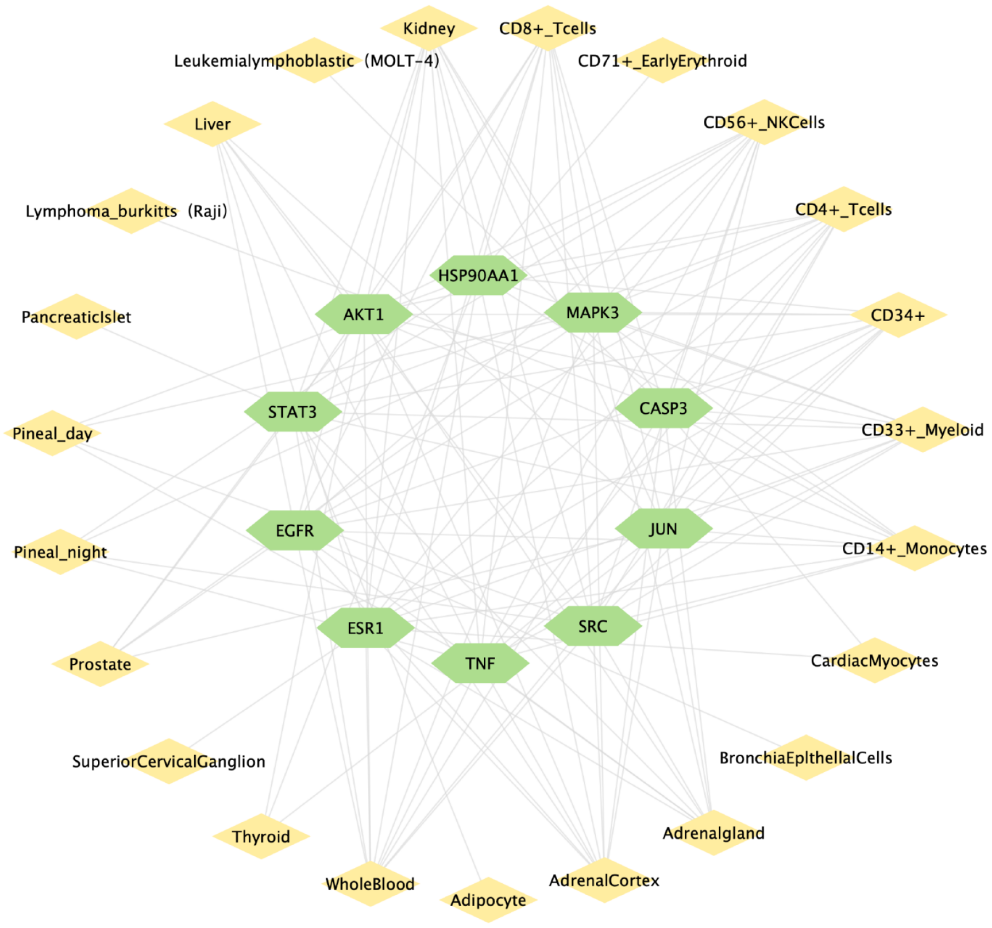

Figure 7 Diagram of the "key target-organ network". The green nodes represent the key targets, while the yellow nodes depict the organs. The edges symbolize the connections between these key targets and organs.

inhibiting oxidative stress and mitochondrial dysfunction through the GSK-3β signaling pathway and plays a protective role in the kidney[42]. The active ingredients in the *Astragalus-Coptis* drug pair are known to have therapeutic effects on DKD.

PPI network analysis indicated that AKT1, EGFR, TNF, SRC, JUN, CASP3, MAPK3, HSP90AA1, STAT3, and ESR1 are the key targets of the *Astragalus-Coptis* drug pair and its active ingredients in the treatment of DKD. Furthermore, the synergistic relationship between these targets is crucial for their therapeutic efficacy. Numerous cell and animal model studies have shown that AKT1, a member of the serine/threonine protein kinase subfamily known as AGC protein kinase, participates in various signaling pathways related to DKD. These intricate signaling pathways underscore the diverse regulatory roles of AKT1 in kidney cell processes affected by DKD and contribute to renal protection[43]. EGFR is a member of the tyrosine kinase ErbB receptor family, whose receptors are widely expressed in mammalian kidneys, including podocytes. Selective removal of EGFR from podocytes can significantly improve the progression of glomerular disease and renal tubulointerstitial fibrosis in DKD, reduce proteinuria, maintain the integrity of podocytes, increase autophagy, and reduce inflammation. EGFR inhibitors may reduce DKD by reducing ROS and ER stress. Quercetin can reduce renal fibrosis *in vitro* and *in vivo* by inhibiting EGFR signaling activation[44,45]. TNF may serve as an autonomous risk factor for the development of chronic kidney disease in patients diagnosed with type 2 diabetes. Elevated levels of TNF inflammatory mediators can exacerbate renal inflammation in individuals suffering from DKD, and it is plausible that inhibition of TNF could mitigate or prevent the onset of DKD. Quercetin inhibits the release of proinflammatory markers such as IL-1β, IL-4, IL-6, and TNF-α, alleviating renal inflammation in DKD[46-48]. SRC is a tyrosine-protein kinase that governs cellular metabolism, survival, and proliferation. Inhibition of SRC kinase significantly upregulates CKIP-1 expression to ameliorate diabetic renal fibrosis. Therefore, targeting SRC may represent a promising strategy for preventing and treating age-related microangiopathy[49]. The transcription factor signal transduction and activator of transcription 3 (STAT3) plays a crucial role in the pathogenesis of renal fibrosis and inflammation. Inhibition of STAT3 impedes the progression and development of DKD[50,51]. Introns 1 and 2 of the ESR1 may contain functionally significant regions associated with the risk of type 2 diabetes or ESRD. ESR1 has favorable effects on blood glucose

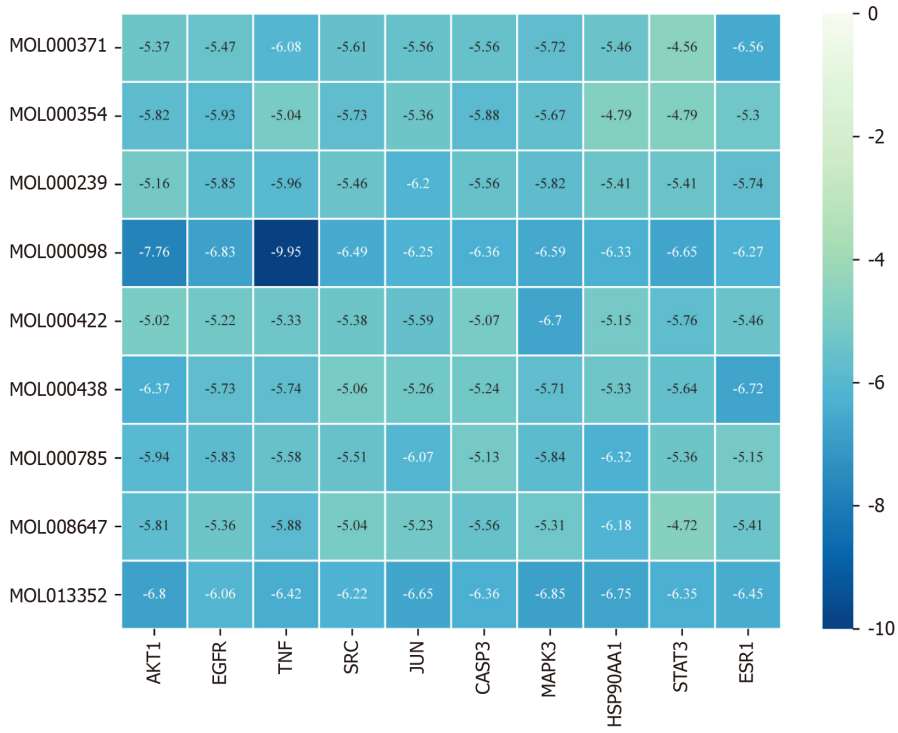

Figure 8 Heatmap of molecular docking binding energies (kcal/mol). The X-axis corresponds to the key target receptor, while the Y-axis represents the core active ingredient. The darker shade of blue in the heatmap indicates a lower binding energy and a stronger binding affinity between the active ingredient and the target.

homeostasis. ESR1 regulates VEGFA expression in adipose tissue, promoting angiogenesis, reducing inflammation, and improving adipose tissue functionality. It confers a protective effect on patients with DKD[52-54]. The above studies suggest that these key targets are closely related to the occurrence and development of DKD and that the core ingredients of the *Astragalus-Coptis* drug pair can regulate these targets to varying degrees.

GO enrichment analysis revealed that the therapeutic effect of the *Astragalus-Coptis* drug pair on DKD primarily involves protein phosphorylation, endoplasmic reticulum (ER) unfolded protein, negative regulation of apoptotic process and inflammatory response, vascular endothelial growth factor receptor signaling pathway, and other cellular BP. Additionally, this effect is associated with various cell components, such as the ER, mitochondria, and exosomes. The MF included protein serine/threonine/tyrosine kinase activity and protein kinase activity. Various studies have demonstrated that protein tyrosine phosphatase nonreceptor type 2 (PTPN2) plays a protective role in DKD by ameliorating metabolic disorders and inhibiting renal STAT phosphorylation-dependent microinflammation[55]. Several factors associated with the pathogenesis of DKD, including hyperglycemia, AGEs, angiotensin II, and various cytokines, have been demonstrated to promote the expression of vascular endothelial growth factor (VEGF) in various cell types. In the early stages of DKD, there is increased VEGF and VEGF2 kidney expression. Inhibiting VEGF-A or its receptor can prevent proteinuria and alleviate glomerular injury, thereby exerting a beneficial effect on kidney changes related to DKD [56,57]. ER stress (ERS) refers to the accumulation of misfolded proteins in cells, which induces cellular stress and regulates cell damage bidirectionally. ERSs are regulated by various signaling pathways and are closely associated with the pathogenesis of DKD[58]. The potential mechanisms by which the *Astragalus-Coptis* drug pair improves DKD are consistent with the GO enrichment results mentioned above.

The KEGG enrichment results included pathways related to the AGE-RAGE signaling pathway in diabetic complications, the Lipid and atherosclerosis, the PI3K-Akt signaling pathway, and the HIF-1 signaling pathway, among others. The active ingredient of the *Astragalus-Coptis* drug pair can enhance the treatment of DKD by targeting the AGE-RAGE signaling pathway, which is involved in diabetic complications, as well as lipid and atherosclerosis. The development of AGEs associated with hyperglycemia plays a pivotal role in the pathogenesis of DKD, and the interaction between AGE receptors (RAGE) and their ligands initiates oxidative stress, chronic inflammation, and fibrosis in renal tissue, ultimately culminating in renal dysfunction. A reduction in AGE levels or inhibition of RAGE is beneficial to DKD in experimental models. The AGE/RAGE signaling pathway elicits ER stress in DKD, and targeting key targets within this pathway holds promise for treating these and other related kidney disorders[59,60]. Additionally, the heightened occurrence of DKD in individuals with diabetes is linked to lipid and atherosclerosis signaling pathway. Dyslipidemia can exacerbate the progression of DKD in patients with DKD. Quercetin may mitigate atherosclerotic lesions by modulating the gut microbiota and reducing atherogenic lipid metabolites[61-63]. By inhibiting the aberrant activation of the PI3K/Akt signaling pathway, it is possible to reduce podocyte apoptosis, restore podocyte homeostasis, alleviate kidney injury, and improve renal function. Quercetin alleviates chronic kidney failure by targeting the PI3K/Akt pathway. Furthermore, activation of the PI3K/Akt signaling pathway plays a crucial role in mediating extracellular matrix accumulation and contributes to the pathogenesis and progression of DKD[64-66]. The above evidence demonstrates that the *Astragalus-*

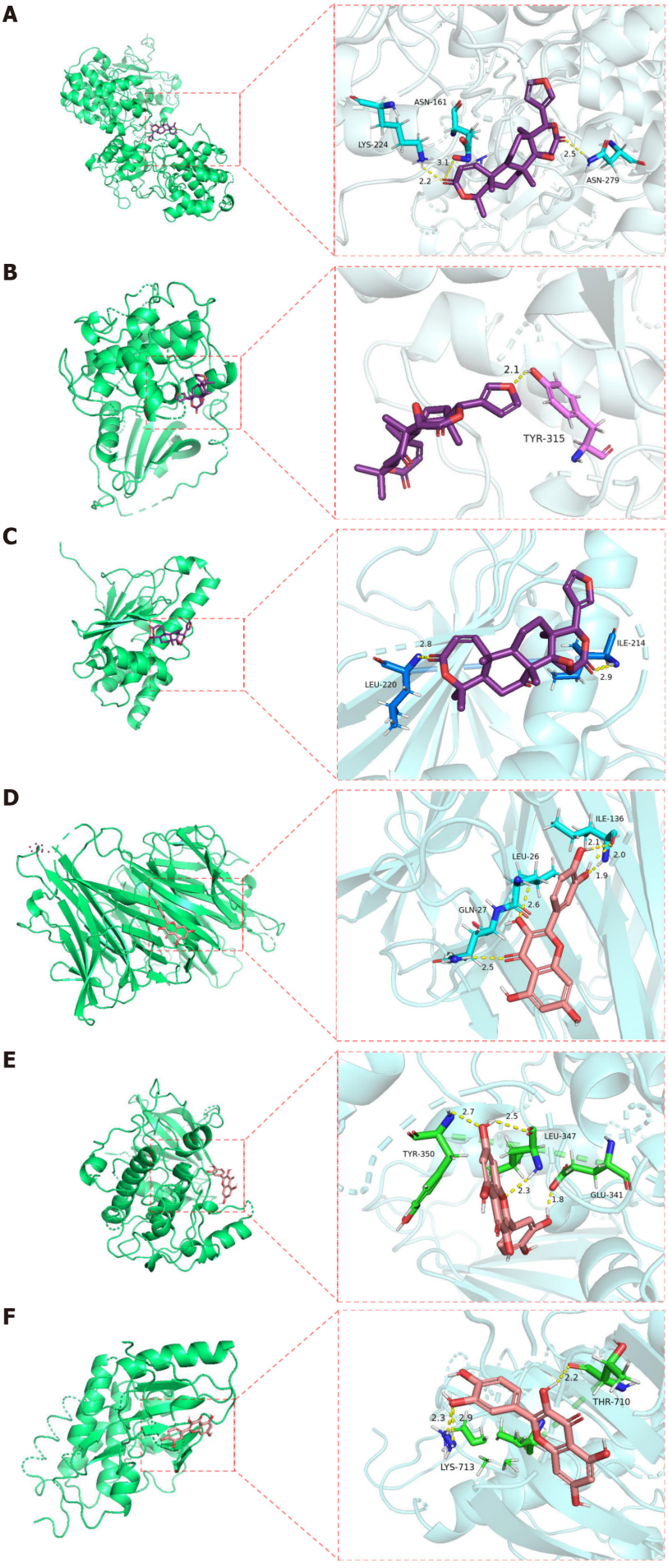
A
ASN-161
LYS-224
3.1
2.2
2.5
ASN-279
B
2.1
TYR-315
C
2.8
LEU-220
ILE-214
2.9
D
ILE-136
2.1
2.0
LEU-26
1.9
GLN-27
2.6
2.5
E
2.7
2.5
LEU-347
TYR-350
2.3
1.8
GLU-341
F
2.2
THR-710
2.3
2.9
LYS-713

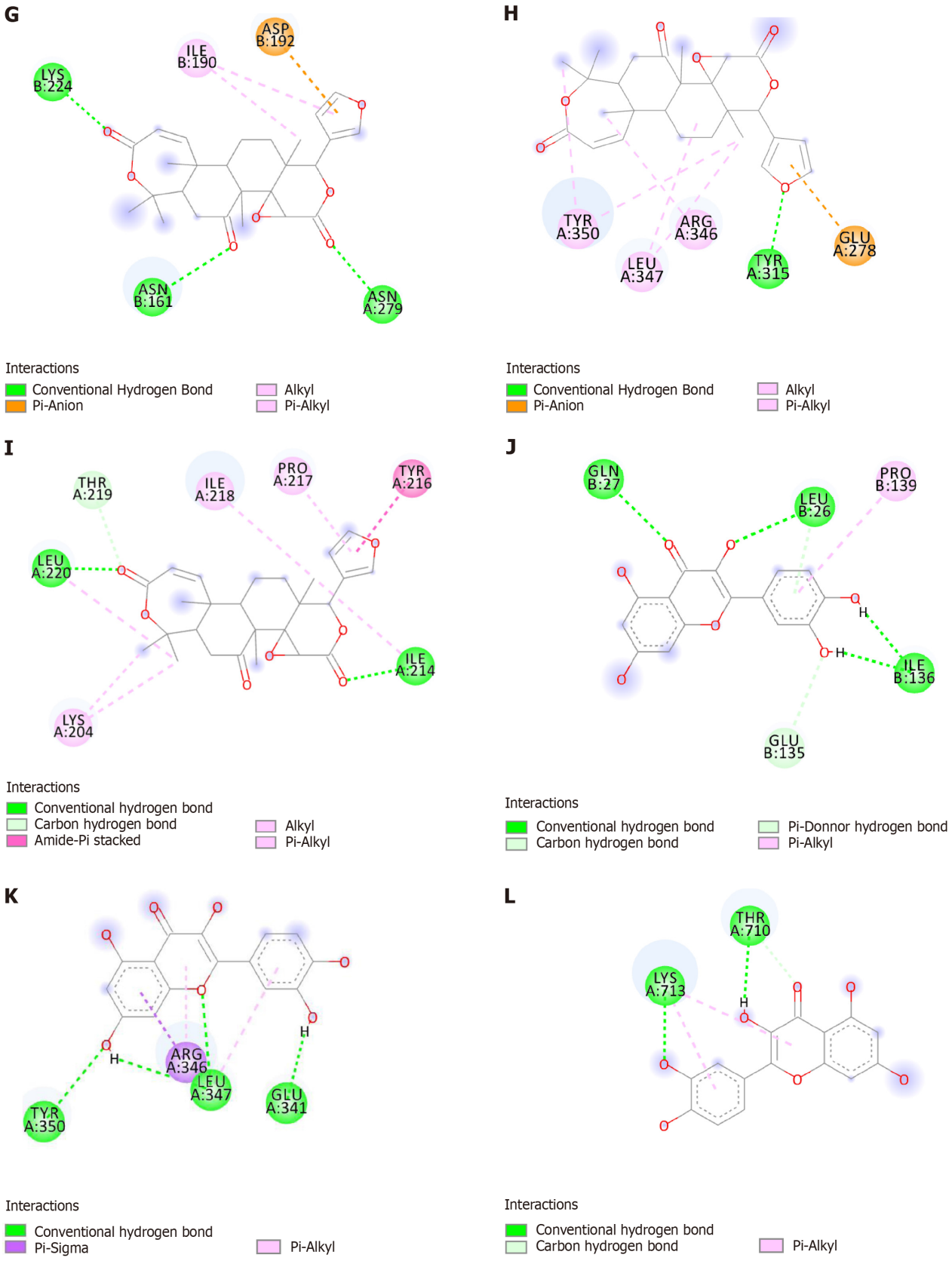

Figure 9 Docking result diagram. A: Obacunone-mitogen-activated protein kinase 3 (MAPK3); B: Obacunone-AKT serine/threonine kinase 1 (AKT1); C: Obacunone-heat shock protein 90 alpha family class A member 1 (HSP90AA1); D: Quercetin-tumor necrosis factor (TNF); E: Quercetin-AKT serine/threonine kinase 1 (AKT1); F: Quercetin-epidermal growth factor receptor (EGFR); G-L: The different types of two-dimensional bonding modes, respectively.

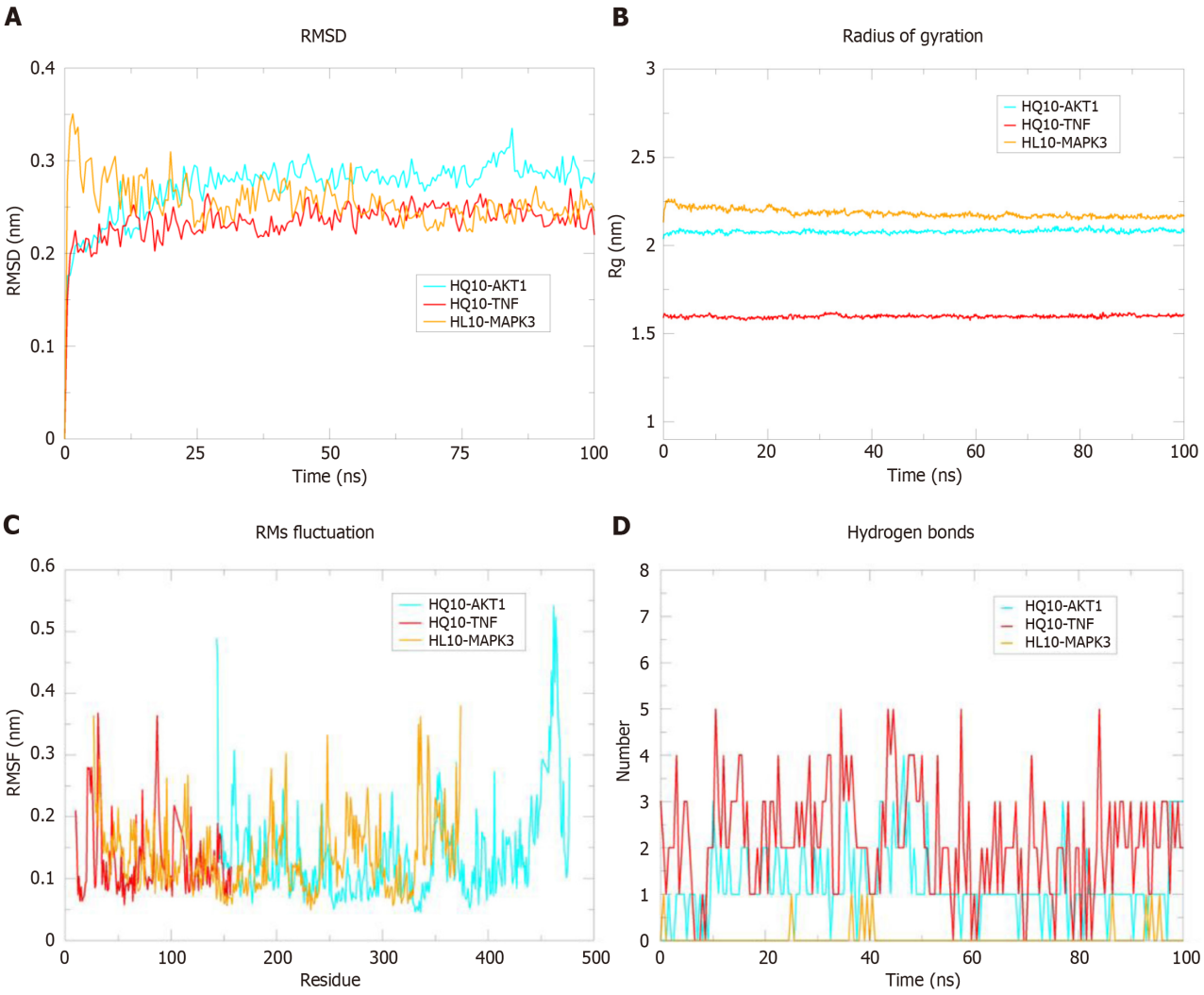

Figure 10 Molecular dynamics simulations of HL10 (obacunone)-mitogen-activated protein kinase 3, HQ10 (quercetin)-AKT serine/threonine kinase 1, and HQ10 (quercetin)-tumor necrosis factor. A: Root mean square deviation (RMSD) plots of HL10-mitogen-activated protein kinase 3 (MAPK3), HQ10-quercetin-AKT serine/threonine kinase 1 (AKT1), and HQ10-tumor necrosis factor (TNF) protein complexes; B: Rg plot of HL10-MAPK3, HQ10-AKT1, and HQ10-TNF protein complexes; C: Root mean square fluctuation (RMSF) plots of HL10-MAPK3, HQ10-AKT1, and HQ10-TNF protein complexes; D: Number of hydrogen bonds in HL10-MAPK3, HQ10-AKT1, and HQ10-TNF protein complexes.

Coptis combination exerts synergistic effects by affecting multiple ingredients, targets, and pathways to improve the treatment of DKD.

Finally, molecular docking was used to evaluate 10 key targets and 9 core active ingredients. The docking results showed binding energies ranging from -4.56 kcal/mol to -9.95 kcal/mol, indicating that all the active ingredients are likely to have good docking ability. The binding energies of the obacunone-MAPK3, quercetin-AKT1, and quercetin-TNF protein complexes were the lowest. It has relatively good docking ability. MD simulations were used to investigate the structural stability of the HL10 (obacunone)-MAPK3, HQ10 (quercetin)-AKT1, and HQ10 (quercetin)-TNF protein complexes. The structures of these protein complexes are very stable at 300 K. The binding free energies of the HQ10-AKT1 and HQ10-TNF protein complexes were -7.44 kcal/mol ± 6.35 kcal/mol and -10.60 kcal/mol ± 9.98 kcal/mol, respectively, which were the lowest among the three groups, indicating good binding activity and structural stability. These findings suggest that these active ingredients, together with their targets, play indispensable roles in DKD treatment. Currently, there is a lack of relevant experimental studies investigating the impact of quercetin on AKT1 and TNF in DKD treatment. However, animal studies have demonstrated that quercetin improves renal function in DKD animals, reduces oxidative stress levels, and alleviates inflammatory responses in the kidneys[67]. Furthermore, a NP study predicted that EGFR is a potential physiological target of quercetin. This finding was confirmed by *in vitro* and *in vivo* experiments, which showed that quercetin inhibits the activation of the EGFR signaling pathway by reducing the phosphorylation of EGFR and ERK1/2, mitigating podocyte apoptosis, and improving DKD[68]. This study utilized NP, molecular docking, and MD to predict that quercetin binds stably to AKT1 and TNF, identifying them as potential therapeutic targets. AKT1 and TNF are implicated in core pathways such as the AGE-RAGE signaling pathway in diabetic complications and the Lipid and atherosclerosis pathway. Consequently, quercetin may modulate these core pathways by targeting AKT1 and TNF, potentially influencing AGEs and lipid metabolism, thereby enhancing the improvement of DKD. The present study, however, has certain limitations. First, the active ingredient and target data

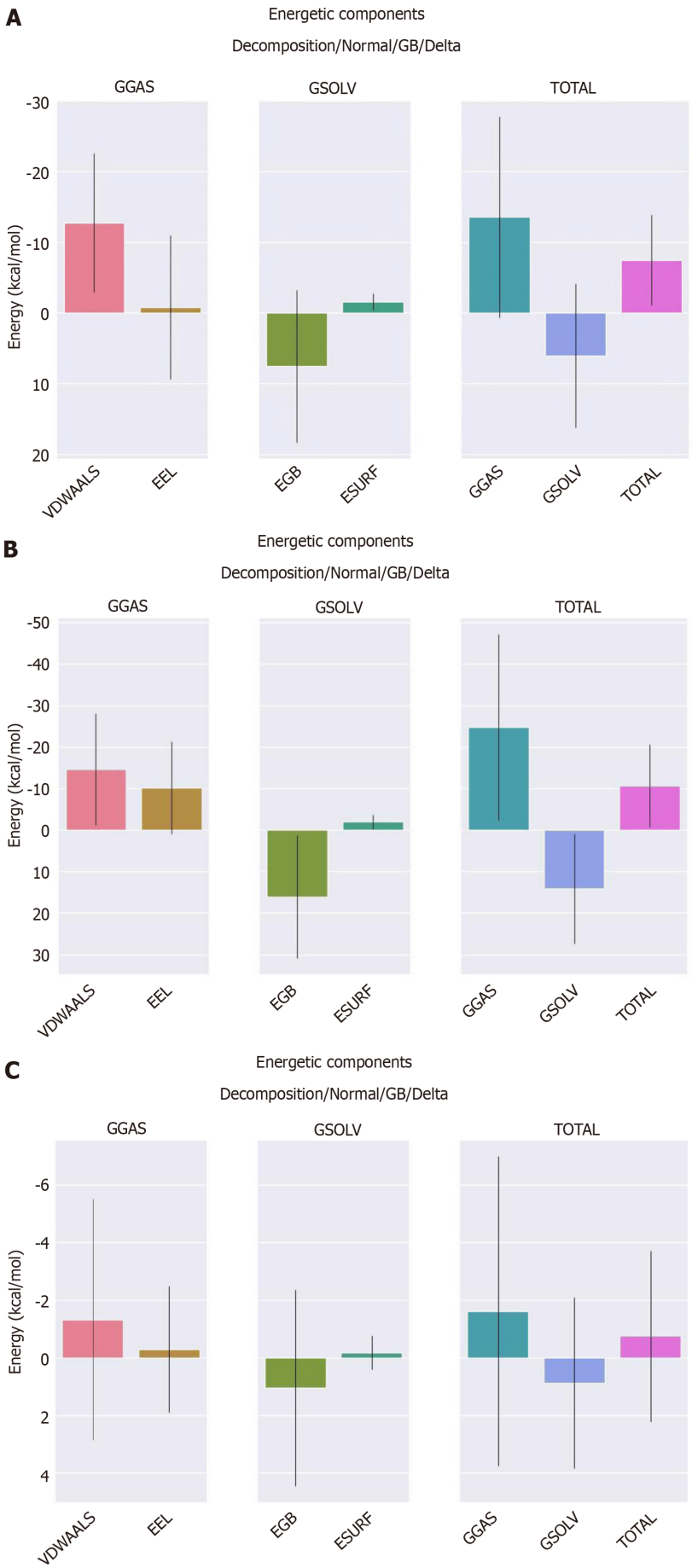

Figure 11 Binding free energy between receptor-ligand protein complexes. A: Binding energy of the HQ10-AKT serine/threonine kinase 1 protein

complex; B: Binding energy of the HQ10-tumor necrosis factor protein complex; C: Binding energy of the HL10-mitogen-activated protein kinase 3 protein complex. EEL: Electrostatic energy; EGB: Polar solvation energy; ESURF: Nonpolar solvation energy; GGAS: Total gas phase free energy; GSOLV: Total solvation free energy (overall total solvation free energy, which is calculated as the sum of total gas phase free energy and total gas phase free energy); VDWAALS: Van der Waals energy.

were obtained from the literature and databases, which may introduce potential biases. Additionally, the reliability and accuracy of predictions heavily rely on the quality of the available data. Therefore, further *in vivo* experiments, *in vitro* experiments and clinical observations are necessary to validate whether the *Astragalus-Coptis* drug pair can effectively improve DKD through the ingredients, targets, and pathways.

CONCLUSION

In summary, this study represents the first systematic exploration of the pharmacological and molecular mechanisms underlying the *Astragalus-Coptis* drug pair treatment for DKD using bioinformatics tools such as NP, molecular docking, and MD simulation. The bioinformatics and computational analysis above demonstrated that quercetin and obacunone are the fundamental active ingredients of the *Astragalus-Coptis* drug pair in DKD treatment. Their mechanisms of action involve the regulation of key targets, such as AKT1, EGFR, TNF, MAPK3, and HSP90AA1, which subsequently modulate various BP, CCs, and MF. Additionally, the *Astragalus-Coptis* drug pair can also intervene in the AGE-RAGE signaling pathway in diabetic complications. Moreover, it can modulate various signaling pathways, such as the Lipid and atherosclerosis pathway and the PI3K-Akt pathway, among others, to enhance glucose and lipid metabolism while reducing atherosclerosis. Furthermore, it potentially mitigates podocyte apoptosis, inhibits inflammation, regulates AGEs and ERS, *etc*, offering therapeutic benefits for DKD. The findings of this study establish a solid theoretical foundation for the use of the *Astragalus-Coptis* drug pair in the treatment of DKD, thereby providing valuable insights for expanding its clinical applications. Moreover, these results are anticipated to serve as a guiding framework for future advanced experimental investigations.

FOOTNOTES

Author contributions: Zhang MY and Zheng SQ participated in the study design and data collection; Zhang MY performed the data analysis; Zhang MY drafted the manuscript; and Zhang MY and Zheng SQ revised the manuscript; All the authors read and approved the final manuscript.

Conflict-of-interest statement: All the authors report having no relevant conflicts of interest for this article.

Open-Access: This article is an open-access article that was selected by an in-house editor and fully peer-reviewed by external reviewers. It is distributed in accordance with the Creative Commons Attribution NonCommercial (CC BY-NC 4.0) license, which permits others to distribute, remix, adapt, build upon this work non-commercially, and license their derivative works on different terms, provided the original work is properly cited and the use is non-commercial. See: https://creativecommons.org/Licenses/by-nc/4.0/

Country of origin: China

ORCID number: Mo-Yan Zhang 0009-0002-2495-790X; Shu-Qin Zheng 0009-0006-2801-5986.

S-Editor: Chen YL
L-Editor: Filipodia
P-Editor: Che XX

REFERENCES

1 **Doshi SM**, Friedman AN. Diagnosis and Management of Type 2 Diabetic Kidney Disease. *Clin J Am Soc Nephrol* 2017; **12**: 1366-1373 [PMID: 28280116 DOI: 10.2215/CJN.11111016]
2 **Alicic RZ**, Rooney MT, Tuttle KR. Diabetic Kidney Disease: Challenges, Progress, and Possibilities. *Clin J Am Soc Nephrol* 2017; **12**: 2032-2045 [PMID: 28522654 DOI: 10.2215/CJN.11491116]
3 **Tuttle KR**, Agarwal R, Alpers CE, Bakris GL, Brosius FC, Kolkhof P, Uribarri J. Molecular mechanisms and therapeutic targets for diabetic kidney disease. *Kidney Int* 2022; **102**: 248-260 [PMID: 35661785 DOI: 10.1016/j.kint.2022.05.012]
4 **Thomas MC**, Brownlee M, Susztak K, Sharma K, Jandeleit-dahm KAM, Zoungas S, Rossing P, Groop P, Cooper ME. Correction: Diabetic kidney disease. *Nat Rev Dis Primers* 2015; **1**: 15070 [DOI: 10.1038/nrdp.2015.70]
5 **Sinha SK**, Nicholas SB. Pathomechanisms of Diabetic Kidney Disease. *J Clin Med* 2023; **12** [PMID: 38068400 DOI: 10.3390/jcm12237349]
6 **Reidy K**, Kang HM, Hostetter T, Susztak K. Molecular mechanisms of diabetic kidney disease. *J Clin Invest* 2014; **124**: 2333-2340 [PMID: 24892707 DOI: 10.1172/JCI72271]

7 **Koye DN**, Magliano DJ, Nelson RG, Pavkov ME. The Global Epidemiology of Diabetes and Kidney Disease. *Adv Chronic Kidney Dis* 2018; **25**: 121-132 [PMID: 29580576 DOI: 10.1053/j.ackd.2017.10.011]

8 **Liyanage T**, Ninomiya T, Jha V, Neal B, Patrice HM, Okpechi I, Zhao MH, Lv J, Garg AX, Knight J, Rodgers A, Gallagher M, Kotwal S, Cass A, Perkovic V. Worldwide access to treatment for end-stage kidney disease: a systematic review. *Lancet* 2015; **385**: 1975-1982 [PMID: 25777665 DOI: 10.1016/S0140-6736(14)61601-9]

9 **Lu Z**, Zhong Y, Liu W, Xiang L, Deng Y. The Efficacy and Mechanism of Chinese Herbal Medicine on Diabetic Kidney Disease. *J Diabetes Res* 2019; **2019**: 2697672 [PMID: 31534972 DOI: 10.1155/2019/2697672]

10 **Liu XJ**, Hu XK, Yang H, Gui LM, Cai ZX, Qi MS, Dai CM. A Review of Traditional Chinese Medicine on Treatment of Diabetic Nephropathy and the Involved Mechanisms. *Am J Chin Med* 2022; **50**: 1739-1779 [PMID: 36222120 DOI: 10.1142/S0192415X22500744]

11 **Xiao Y**, Liu Y, Yu K, Zhou L, Bi J, Cheng J, Li F, Luo R, Zhao X. The effect of chinese herbal medicine on albuminuria levels in patients with diabetic nephropathy: a systematic review and meta-analysis. *Evid Based Complement Alternat Med* 2013; **2013**: 937549 [PMID: 24062795 DOI: 10.1155/2013/937549]

12 **Shi Y**, Shi X, Zhao M, Ma S, Zhang Y. Pharmacological potential of Astragali Radix for the treatment of kidney diseases. *Phytomedicine* 2024; **123**: 155196 [PMID: 37952410 DOI: 10.1016/j.phymed.2023.155196]

13 **Hu S**, Wang J, Liu E, Zhang X, Xiang J, Li W, Wei P, Zeng J, Zhang Y, Ma X. Protective effect of berberine in diabetic nephropathy: A systematic review and meta-analysis revealing the mechanism of action. *Pharmacol Res* 2022; **185**: 106481 [PMID: 36195307 DOI: 10.1016/j.phrs.2022.106481]

14 **Li X**, Liu Z, Liao J, Chen Q, Lu X, Fan X. Network pharmacology approaches for research of Traditional Chinese Medicines. *Chin J Nat Med* 2023; **21**: 323-332 [PMID: 37245871 DOI: 10.1016/S1875-5364(23)60429-7]

15 **Zhao L**, Zhang H, Li N, Chen J, Xu H, Wang Y, Liang Q. Network pharmacology, a promising approach to reveal the pharmacology mechanism of Chinese medicine formula. *J Ethnopharmacol* 2023; **309**: 116306 [PMID: 36858276 DOI: 10.1016/j.jep.2023.116306]

16 **Meng XY**, Zhang HX, Mezei M, Cui M. Molecular docking: a powerful approach for structure-based drug discovery. *Curr Comput Aided Drug Des* 2011; **7**: 146-157 [PMID: 21534921 DOI: 10.2174/157340911795677602]

17 **De Vivo M**, Masetti M, Bottegoni G, Cavalli A. Role of Molecular Dynamics and Related Methods in Drug Discovery. *J Med Chem* 2016; **59**: 4035-4061 [PMID: 26807648 DOI: 10.1021/acs.jmedchem.5b01684]

18 **Ru J**, Li P, Wang J, Zhou W, Li B, Huang C, Li P, Guo Z, Tao W, Yang Y, Xu X, Li Y, Wang Y, Yang L. TCMSP: a database of systems pharmacology for drug discovery from herbal medicines. *J Cheminform* 2014; **6**: 13 [PMID: 24735618 DOI: 10.1186/1758-2946-6-13]

19 **Zhang Y**, Li Z, Wei J, Kong L, Song M, Zhang Y, Xiao X, Cao H, Jin Y. Network pharmacology and molecular docking reveal the mechanism of Angelica dahurica against Osteosarcoma. *Medicine (Baltimore)* 2022; **101**: e31055 [PMID: 36343039 DOI: 10.1097/MD.0000000000031055]

20 **Daina A**, Michielin O, Zoete V. SwissADME: a free web tool to evaluate pharmacokinetics, drug-likeness and medicinal chemistry friendliness of small molecules. *Sci Rep* 2017; **7**: 42717 [PMID: 28256516 DOI: 10.1038/srep42717]

21 **Stelzer G**, Rosen N, Plaschkes I, Zimmerman S, Twik M, Fishilevich S, Stein TI, Nudel R, Lieder I, Mazor Y, Kaplan S, Dahary D, Warshawsky D, Guan-Golan Y, Kohn A, Rappaport N, Safran M, Lancet D. The GeneCards Suite: From Gene Data Mining to Disease Genome Sequence Analyses. *Curr Protoc Bioinformatics* 2016; **54**: 1.30.1-1.30.33 [PMID: 27322403 DOI: 10.1002/cpbi.5]

22 **Amberger JS**, Bocchini CA, Schiettecatte F, Scott AF, Hamosh A. OMIM.org: Online Mendelian Inheritance in Man (OMIM®), an online catalog of human genes and genetic disorders. *Nucleic Acids Res* 2015; **43**: D789-D798 [PMID: 25428349 DOI: 10.1093/nar/gku1205]

23 **Piñero J**, Saüch J, Sanz F, Furlong LI. The DisGeNET cytoscape app: Exploring and visualizing disease genomics data. *Comput Struct Biotechnol J* 2021; **19**: 2960-2967 [PMID: 34136095 DOI: 10.1016/j.csbj.2021.05.015]

24 **Barrett T**, Wilhite SE, Ledoux P, Evangelista C, Kim IF, Tomashevsky M, Marshall KA, Phillippy KH, Sherman PM, Holko M, Yefanov A, Lee H, Zhang N, Robertson CL, Serova N, Davis S, Soboleva A. NCBI GEO: archive for functional genomics data sets--update. *Nucleic Acids Res* 2013; **41**: D991-D995 [PMID: 23193258 DOI: 10.1093/nar/gks1193]

25 **Wang Y**, Yuan Y, Wang W, He Y, Zhong H, Zhou X, Chen Y, Cai XJ, Liu LQ. Mechanisms underlying the therapeutic effects of Qingfeiyin in treating acute lung injury based on GEO datasets, network pharmacology and molecular docking. *Comput Biol Med* 2022; **145**: 105454 [PMID: 35367781 DOI: 10.1016/j.compbiomed.2022.105454]

26 **Shannon P**, Markiel A, Ozier O, Baliga NS, Wang JT, Ramage D, Amin N, Schwikowski B, Ideker T. Cytoscape: a software environment for integrated models of biomolecular interaction networks. *Genome Res* 2003; **13**: 2498-2504 [PMID: 14597658 DOI: 10.1101/gr.1239303]

27 **Szklarczyk D**, Kirsch R, Koutrouli M, Nastou K, Mehryary F, Hachilif R, Gable AL, Fang T, Doncheva NT, Pyysalo S, Bork P, Jensen LJ, von Mering C. The STRING database in 2023: protein-protein association networks and functional enrichment analyses for any sequenced genome of interest. *Nucleic Acids Res* 2023; **51**: D638-D646 [PMID: 36370105 DOI: 10.1093/nar/gkac1000]

28 **Zhao J**, Lin F, Liang G, Han Y, Xu N, Pan J, Luo M, Yang W, Zeng L. Exploration of the Molecular Mechanism of Polygonati Rhizoma in the Treatment of Osteoporosis Based on Network Pharmacology and Molecular Docking. *Front Endocrinol (Lausanne)* 2021; **12**: 815891 [PMID: 35069454 DOI: 10.3389/fendo.2021.815891]

29 **Sherman BT**, Hao M, Qiu J, Jiao X, Baseler MW, Lane HC, Imamichi T, Chang W. DAVID: a web server for functional enrichment analysis and functional annotation of gene lists (2021 update). *Nucleic Acids Res* 2022; **50**: W216-W221 [PMID: 35325185 DOI: 10.1093/nar/gkac194]

30 **Kanehisa M**, Furumichi M, Sato Y, Kawashima M, Ishiguro-Watanabe M. KEGG for taxonomy-based analysis of pathways and genomes. *Nucleic Acids Res* 2023; **51**: D587-D592 [PMID: 36300620 DOI: 10.1093/nar/gkac963]

31 **Wu C**, Orozco C, Boyer J, Leglise M, Goodale J, Batalov S, Hodge CL, Haase J, Janes J, Huss JW 3rd, Su AI. BioGPS: an extensible and customizable portal for querying and organizing gene annotation resources. *Genome Biol* 2009; **10**: R130 [PMID: 19919682 DOI: 10.1186/gb-2009-10-11-r130]

32 **Liu L**, Jiao Y, Yang M, Wu L, Long G, Hu W. Network Pharmacology, Molecular Docking and Molecular Dynamics to Explore the Potential Immunomodulatory Mechanisms of Deer Antler. *Int J Mol Sci* 2023; **24** [PMID: 37373516 DOI: 10.3390/ijms241210370]

33 **Valdés-Tresanco MS**, Valdés-Tresanco ME, Valiente PA, Moreno E. gmx_MMPBSA: A New Tool to Perform End-State Free Energy Calculations with GROMACS. *J Chem Theory Comput* 2021; **17**: 6281-6291 [PMID: 34586825 DOI: 10.1021/acs.jctc.1c00645]

34 **Dong Y**, Zhao Q, Wang Y. Network pharmacology-based investigation of potential targets of astragalus membranaceous-angelica sinensis compound acting on diabetic nephropathy. *Sci Rep* 2021; **11**: 19496 [PMID: 34593896 DOI: 10.1038/s41598-021-98925-6]

35 **Mukherjee S**, Balius TE, Rizzo RC. Docking validation resources: protein family and ligand flexibility experiments. *J Chem Inf Model* 2010; **50**: 1986-2000 [PMID: 21033739 DOI: 10.1021/ci1001982]

36 **Lobanov MY**, Bogatyreva NS, Galzitskaya OV. Radius of gyration as an indicator of protein structure compactness. *Mol Biol* 2008; **42**: 623-628 [DOI: 10.1134/S0026893308040195]

37 **Li Z**, Deng H, Guo X, Yan S, Lu C, Zhao Z, Feng X, Li Q, Wang J, Zeng J, Ma X. Effective dose/duration of natural flavonoid quercetin for treatment of diabetic nephropathy: A systematic review and meta-analysis of rodent data. *Phytomedicine* 2022; **105**: 154348 [PMID: 35908521 DOI: 10.1016/j.phymed.2022.154348]

38 **Kalai FZ**, Boulaaba M, Ferdousi F, Isoda H. Effects of Isorhamnetin on Diabetes and Its Associated Complications: A Review of In Vitro and In Vivo Studies and a Post Hoc Transcriptome Analysis of Involved Molecular Pathways. *Int J Mol Sci* 2022; **23** [PMID: 35054888 DOI: 10.3390/ijms23020704]

39 **Feng Q**, Yang Y, Qiao Y, Zheng Y, Yu X, Liu F, Wang H, Zheng B, Pan S, Ren K, Liu D, Liu Z. Quercetin Ameliorates Diabetic Kidney Injury by Inhibiting Ferroptosis *via* Activating Nrf2/HO-1 Signaling Pathway. *Am J Chin Med* 2023; **51**: 997-1018 [PMID: 37046368 DOI: 10.1142/S0192415X23500465]

40 **Dhanya R**. Quercetin for managing type 2 diabetes and its complications, an insight into multitarget therapy. *Biomed Pharmacother* 2022; **146**: 112560 [PMID: 34953390 DOI: 10.1016/j.biopha.2021.112560]

41 **Yuan L**, Tu D, Ye X, Wu J. Hypoglycemic and hypocholesterolemic effects of Coptis chinensis franch inflorescence. *Plant Foods Hum Nutr* 2006; **61**: 139-144 [PMID: 17031605 DOI: 10.1007/s11130-006-0023-7]

42 **Zhou J**, Wang T, Wang H, Jiang Y, Peng S. Obacunone attenuates high glucose-induced oxidative damage in NRK-52E cells by inhibiting the activity of GSK-3β. *Biochem Biophys Res Commun* 2019; **513**: 226-233 [PMID: 30954216 DOI: 10.1016/j.bbrc.2019.03.201]

43 **Heljić M**, Brazil DP. Protein kinase B/Akt regulation in diabetic kidney disease. *Front Biosci (Schol Ed)* 2011; **3**: 98-104 [PMID: 21196360 DOI: 10.2741/s135]

44 **Li Y**, Pan Y, Cao S, Sasaki K, Wang Y, Niu A, Fan X, Wang S, Zhang MZ, Harris RC. Podocyte EGFR Inhibits Autophagy Through Upregulation of Rubicon in Type 2 Diabetic Nephropathy. *Diabetes* 2021; **70**: 562-576 [PMID: 33239448 DOI: 10.2337/db20-0660]

45 **Wang Q**, Wang F, Li X, Ma Z, Jiang D. Quercetin inhibits the amphiregulin/EGFR signaling-mediated renal tubular epithelial-mesenchymal transition and renal fibrosis in obstructive nephropathy. *Phytother Res* 2023; **37**: 111-123 [PMID: 36221860 DOI: 10.1002/ptr.7599]

46 **Mansoor G**, Tahir M, Maqbool T, Abbasi SQ, Hadi F, Shakoori TA, Akhtar S, Rafiq M, Ashraf M, Ullah I. Increased Expression of Circulating Stress Markers, Inflammatory Cytokines and Decreased Antioxidant Level in Diabetic Nephropathy. *Medicina (Kaunas)* 2022; **58** [PMID: 36363561 DOI: 10.3390/medicina58111604]

47 **Ansari P**, Choudhury ST, Seidel V, Rahman AB, Aziz MA, Richi AE, Rahman A, Jafrin UH, Hannan JMA, Abdel-Wahab YHA. Therapeutic Potential of Quercetin in the Management of Type-2 Diabetes Mellitus. *Life (Basel)* 2022; **12** [PMID: 36013325 DOI: 10.3390/life12081146]

48 **Yeo ES**, Hwang JY, Park JE, Choi YJ, Huh KB, Kim WY. Tumor necrosis factor (TNF-alpha) and C-reactive protein (CRP) are positively associated with the risk of chronic kidney disease in patients with type 2 diabetes. *Yonsei Med J* 2010; **51**: 519-525 [PMID: 20499416 DOI: 10.3349/ymj.2010.51.4.519]

49 **Yang Y**, Xiao H, Lin Z, Chen R, Li S, Li C, Sun X, Hei Z, Gong W, Huang H. The ubiquitination of CKIP-1 mediated by Src aggravates diabetic renal fibrosis (original article). *Biochem Pharmacol* 2022; **206**: 115339 [PMID: 36347273 DOI: 10.1016/j.bcp.2022.115339]

50 **Ajay AK**, Zhao L, Vig S, Fujiwara M, Thakurela S, Jadhav S, Cho A, Chiu IJ, Ding Y, Ramachandran K, Mithal A, Bhatt A, Chaluvadi P, Gupta MK, Shah SI, Sabbisetti VS, Waaga-Gasser AM, Frank DA, Murugaiyan G, Bonventre JV, Hsiao LL. Deletion of STAT3 from Foxd1 cell population protects mice from kidney fibrosis by inhibiting pericytes trans-differentiation and migration. *Cell Rep* 2022; **38**: 110473 [PMID: 35263586 DOI: 10.1016/j.celrep.2022.110473]

51 **Zheng C**, Huang L, Luo W, Yu W, Hu X, Guan X, Cai Y, Zou C, Yin H, Xu Z, Liang G, Wang Y. Inhibition of STAT3 in tubular epithelial cells prevents kidney fibrosis and nephropathy in STZ-induced diabetic mice. *Cell Death Dis* 2019; **10**: 848 [PMID: 31699972 DOI: 10.1038/s41419-019-2085-0]

52 **Gregorio KCR**, Laurindo CP, Machado UF. Estrogen and Glycemic Homeostasis: The Fundamental Role of Nuclear Estrogen Receptors ESR1/ESR2 in Glucose Transporter GLUT4 Regulation. *Cells* 2021; **10** [PMID: 33430527 DOI: 10.3390/cells10010099]

53 **Fatima LA**, Campello RS, Santos RS, Freitas HS, Frank AP, Machado UF, Clegg DJ. Estrogen receptor 1 (ESR1) regulates VEGFA in adipose tissue. *Sci Rep* 2017; **7**: 16716 [PMID: 29196658 DOI: 10.1038/s41598-017-16686-7]

54 **Gallagher CJ**, Keene KL, Mychaleckyj JC, Langefeld CD, Hirschhorn JN, Henderson BE, Gordon CJ, Freedman BI, Rich SS, Bowden DW, Sale MM. Investigation of the estrogen receptor-alpha gene with type 2 diabetes and/or nephropathy in African-American and European-American populations. *Diabetes* 2007; **56**: 675-684 [PMID: 17327435 DOI: 10.2337/db06-0303]

55 **Li Y**, Zhou H, Li Y, Han L, Song M, Chen F, Shang G, Wang D, Wang Z, Zhang W, Zhong M. PTPN2 improved renal injury and fibrosis by suppressing STAT-induced inflammation in early diabetic nephropathy. *J Cell Mol Med* 2019; **23**: 4179-4195 [PMID: 30955247 DOI: 10.1111/jcmm.14304]

56 **Yang J**, Liu Z. Mechanistic Pathogenesis of Endothelial Dysfunction in Diabetic Nephropathy and Retinopathy. *Front Endocrinol (Lausanne)* 2022; **13**: 816400 [PMID: 35692405 DOI: 10.3389/fendo.2022.816400]

57 **Chawla A**, Chawla R, Jaggi S. Microvasular and macrovascular complications in diabetes mellitus: Distinct or continuum? *Indian J Endocrinol Metab* 2016; **20**: 546-551 [PMID: 27366724 DOI: 10.4103/2230-8210.183480]

58 **Zhang R**, Bian C, Gao J, Ren H. Endoplasmic reticulum stress in diabetic kidney disease: adaptation and apoptosis after three UPR pathways. *Apoptosis* 2023; **28**: 977-996 [PMID: 37285056 DOI: 10.1007/s10495-023-01858-w]

59 **Sanajou D**, Ghorbani Haghjo A, Argani H, Aslani S. AGE-RAGE axis blockade in diabetic nephropathy: Current status and future directions. *Eur J Pharmacol* 2018; **833**: 158-164 [PMID: 29883668 DOI: 10.1016/j.ejphar.2018.06.001]

60 **Pathomthongtaweechai N**, Chutipongtanate S. AGE/RAGE signaling-mediated endoplasmic reticulum stress and future prospects in non-coding RNA therapeutics for diabetic nephropathy. *Biomed Pharmacother* 2020; **131**: 110655 [PMID: 32853909 DOI: 10.1016/j.biopha.2020.110655]

61 **Chen SC**, Tseng CH. Dyslipidemia, kidney disease, and cardiovascular disease in diabetic patients. *Rev Diabet Stud* 2013; **10**: 88-100 [PMID: 24380085 DOI: 10.1900/RDS.2013.10.88]

62 **Morton J**, Zoungas S, Li Q, Patel AA, Chalmers J, Woodward M, Celermajer DS, Beulens JW, Stolk RP, Glasziou P, Ng MK; ADVANCE Collaborative Group. Low HDL cholesterol and the risk of diabetic nephropathy and retinopathy: results of the ADVANCE study. *Diabetes Care* 2012; **35**: 2201-2206 [PMID: 22891258 DOI: 10.2337/dc12-0306]

63 **Nie J**, Zhang L, Zhao G, Du X. Quercetin reduces atherosclerotic lesions by altering the gut microbiota and reducing atherogenic lipid metabolites. *J Appl Microbiol* 2019; **127**: 1824-1834 [PMID: 31509634 DOI: 10.1111/jam.14441]

64 **Nie Y**, Fu C, Zhang H, Zhang M, Xie H, Tong X, Li Y, Hou Z, Fan X, Yan M. Celastrol slows the progression of early diabetic nephropathy in

rats *via* the PI3K/AKT pathway. *BMC Complement Med Ther* 2020; **20**: 321 [PMID: 33097050 DOI: 10.1186/s12906-020-03050-y]

65 **Zhang Y**, Chen X, Yuan L, Zhang Y, Wu J, Guo N, Chen X, Liu J. Down-regulation of IRAK1 attenuates podocyte apoptosis in diabetic nephropathy through PI3K/Akt signaling pathway. *Biochem Biophys Res Commun* 2018; **506**: 529-535 [PMID: 30361091 DOI: 10.1016/j.bbrc.2018.09.175]

66 **Tu H**, Ma D, Luo Y, Tang S, Li Y, Chen G, Wang L, Hou Z, Shen C, Lu H, Zhuang X, Zhang L. Quercetin alleviates chronic renal failure by targeting the PI3k/Akt pathway. *Bioengineered* 2021; **12**: 6538-6558 [PMID: 34528858 DOI: 10.1080/21655979.2021.1973877]

67 **Hu T**, Yue J, Tang Q, Cheng KW, Chen F, Peng M, Zhou Q, Wang M. The effect of quercetin on diabetic nephropathy (DN): a systematic review and meta-analysis of animal studies. *Food Funct* 2022; **13**: 4789-4803 [PMID: 35416188 DOI: 10.1039/d1fo03958j]

68 **Liu Y**, Li Y, Xu L, Shi J, Yu X, Wang X, Li X, Jiang H, Yang T, Yin X, Du L, Lu Q. Quercetin Attenuates Podocyte Apoptosis of Diabetic Nephropathy Through Targeting EGFR Signaling. *Front Pharmacol* 2021; **12**: 792777 [PMID: 35069207 DOI: 10.3389/fphar.2021.792777]

Published by **Baishideng Publishing Group Inc**
7041 Koll Center Parkway, Suite 160, Pleasanton, CA 94566, USA
Telephone: +1-925-3991568
E-mail: office@baishideng.com
Help Desk: https://www.f6publishing.com/helpdesk
https://www.wjgnet.com

© 2024 Baishideng Publishing Group Inc. All rights reserved.